Rhythms of Transcription in Field-Grown Sugarcane Are Highly Organ Specific

Luíza Lane Barros Dantas[1,2], Natalia Oliveira de Lima[1], Cícero Alves-Lima[1], Milton Yutaka Nishiyama-Jr[1,3], Monalisa Sampaio Carneiro[4], Glaucia Mendes Souza[1], Carlos Takeshi Hotta[1*]

1 Departamento de Bioquímica, Instituto de Química, Universidade de São Paulo, São Paulo, SP, 05508-000, Brazil

2 Present address: Max Planck Institute for Molecular Plant Physiology, Potsdam-Golm, 14476, Germany

3 Present address: Laboratório Especial de Toxicologia Aplicada, Instituto Butantan, São Paulo, SP, 05503-900, Brazil

4 Departamento de Biotecnologia e Produção Vegetal e Animal, Centro de Ciências Agrárias, Universidade Federal de São Carlos, São Carlos, SP, 13600-970, Brazil.

* corresponding author: hotta@iq.usp.br

Running Title: Organ-specific rhythms of transcription in sugarcane

Total word count: 5920

Introduction word count: 940

Materials and Methods word count: 918

Results word count: 2230

Discussion word count: 1787

Acknowledgements word count: 45

Number of Figures (all coloured): 4

Number of Supplemental Figures (all coloured): 10

Number of Supplemental tables: 1

Summary

- We investigated whether different specialized organs in field-grown sugarcane follow the same temporal rhythms in transcription.
- We assayed the transcriptomes of three organs during the day: leaf, a source organ; internodes 1 and 2, sink organs focused on cell division and elongation; and internode 5, a sink organ focused on sucrose storage.
- The leaf had twice as many rhythmic transcripts (>68%) as internodes, and the rhythmic transcriptomes of the two types of internodes were more similar to each other than to those of the leaves. More transcripts were rhythmic under field conditions than under circadian conditions and most of their peaks were during the day. Among the transcripts that were considered expressed in all three organs, only 7.4% showed the same rhythmic time course pattern. The central oscillators of these three organs — the networks that generate circadian rhythms — had similar dynamics with different amplitudes.
- The differences between the rhythmic transcriptomes in circadian conditions and field conditions highlight the importance of field experiments to understand how the plant circadian clock works *in natura*. The highly specialized nature of the rhythmic transcriptomes in sugarcane organs probably arises from amplitude differences in the circadian clock and different sensitivities to environmental cues.

Keywords: circadian clock, field conditions, natural conditions, organ-specific, rhythms, Saccharum, sugarcane, tissue-specific

Introduction

The circadian clock is an endogenous signaling network that allows organisms to adapt to rhythmically changing environments. Plants with a circadian clock synchronized with environmental rhythms accumulate more biomass and have better fitness than plants with defective or no circadian clocks (Green *et al.*, 2002; Dodd *et al.*, 2005). In crops, changes in the circadian clock have been indirectly selected through traditional breeding to change photoperiodic responses, such as the transition to flowering. For example, the circadian clocks of European tomatoes have longer periods than those of native American tomatoes, as such periods allow these crops to adapt better to the long summer days occurring at the high latitudes of much of Europe (Muller *et al.*, 2016). Similarly, some genotypes of *Hordeum vulgare* L. (barley) and *Triticum aestivum* L. (wheat) carry mutations in their circadian clock genes that reduce flowering induced by photoperiodic triggers, allowing cultivation in higher latitudes in Europe (Turner *et al.*, 2005; Gawroński *et al.*, 2014).

The circadian clock is conceptually divided into three associated parts: the *Input Pathways*, the *Central Oscillator*, and the *Output Pathways*. The *Input Pathways* detect entraining cues that keep the circadian clock continuously synchronized to the environment. In plants, these cues include light, temperature, and sugar levels (Oakenfull & Davis, 2017; Frank *et al.*, 2018; Webb *et al.*, 2019). The *Central Oscillator* is a series of interlocking transcriptional-translational feedback loops that can generate 24-h rhythms independently of the environment. In *Arabidopsis thaliana* (L.) Heynh. (Arabidopsis), one loop, called the morning loop, starts with the light induction of *CIRCADIAN CLOCK ASSOCIATED1* (*CCA1*) and *LATE ELONGATED HYPOCOTYL* (*LHY*) at dawn. Next, *PSEUDO-RESPONSE REGULATOR7* (*PRR7*) and *PRR9* are activated by CCA1 and LHY. In turn, *CCA1* and *LHY* are repressed by PRR7 and PRR9. In the core loop, CCA1 and LHY are repressed, and this represses *TIME FOR CAB EXPRESSION1* (*TOC1*), also known as *PRR1*. During the night, TOC1 forms an interaction known as the evening loop with the EVENING COMPLEX (EC). The EC is a protein complex formed by EARLY FLOWERING3 (ELF3), ELF4, and LUX ARRHYTHMO (LUX) that also inhibits the expression of *PRR7* and *PRR9* the next morning. Other essential components of the oscillator include GIGANTEA (GI), REVEILLE8 (RVE8), and CCA1 HIKING EXPEDITION (CHE) (Hsu *et al.*, 2013; Millar, 2016; Henriques *et al.*, 2018; Webb *et al.*, 2019). The *Output Pathways* transduce the temporal information generated by the interaction between the *Central Oscillator* and the *Input Pathways* to a plethora of biochemical pathways. The circadian clock thus

has a broad impact throughout the plant, regulating processes such as photosynthesis, cell elongation, stomata opening, and flowering (Hotta *et al.*, 2007).

Even though the plant circadian clock is highly conserved, there are a few differences between the circadian clocks of Arabidopsis and grasses (Poales). For instance, *CCA1* is absent from grasses, as it was created by a duplication exclusive to Brassicaceae. The grass PRRs consist of TOC1, PRR37, PRR73, PRR59, and PRR95, and it is not clear whether they have the same functions as their Arabidopsis counterparts, even though they are capable of complementing Arabidopsis mutations (Kusakina *et al.*, 2015; Calixto *et al.*, 2015). In sugarcane, a highly polyploid crop that accumulates sucrose in the culm, the circadian clock has high-amplitude rhythms and regulates a large proportion of the leaf transcriptome (>30%) (Hotta *et al.*, 2013; Glassop & Rae, 2019).

Most research to date on plant circadian rhythms has been done in controlled conditions, inside a growth room or growth chamber. Under such circumstances, plants can be grown either under circadian conditions, in which they are kept under constant abiotic conditions as a means to separate endogenous rhythms from rhythms driven by the environment, or under diel conditions, in which they are subjected to abiotic rhythms such as light/dark and warm/cold. Abiotic changes in controlled conditions are usually stepwise, in contrast to the gradients found in natural or field conditions, which can lead to significant changes in plant physiology (Shalit-Kaneh *et al.*, 2018; Annunziata *et al.*, 2018; Song *et al.*, 2018). For example, simulations of natural conditions in growth chambers showed that the clock-controlled gene *FLOWERING LOCUS T* (*FT*) has a different phase under such conditions than it does under controlled conditions (Song *et al.*, 2018), highlighting the need for adjustments in the current models to reflect events in natural conditions. In another study, the period and phase of the circadian clock affected shoot and rosette branch numbers in multiple Arabidopsis mutants in natural, but not controlled, conditions (Rubin *et al.*, 2017). Finally, the rice mutant *osgi*, which has a late-flowering phenotype in controlled conditions, flowered at the same time as the wild type in field conditions (Izawa *et al.*, 2011).

Only two plant species have had their rhythmic transcripts identified in field conditions: rice and pineapple (Izawa et al., 2011; Nagano et al., 2012; Matsuzaki et al., 2015; Ming et al., 2015). However, these studies focused on the leaves. To better understand how the plant circadian clock regulates transcription under natural conditions in different organs, we measured transcription in three organs of field-grown sugarcane

grown during the day. We harvested leaf +1 (L1), a source organ, and two sink organs: internodes 1 and 2 (I1), organs focused on cell division and cell elongation that includes the shoot apical meristem; and internode 5 (I5), an organ focused on sucrose accumulation. We describe in detail one cycle (24 h) with 14 time points, starting 2 h before dawn. This approach allowed us to obtain a better resolution to describe transcripts with fast dynamics. We found that the rhythmic transcripts of the L1, I1, and I5 are widely specialized and likely to respond differently to environmental cues.

Materials and Methods

Plant growth and harvesting

Commercial sugarcane (*Saccharum* hybrid SP80-3280) was planted in a field in Araras, Brazil (22°18'41.0"S, 47°23'05.0"W, at an altitude of 611 m), in April 2012 (autumn) (Fig. S1). The soil on the site was a Typic Eutroferric Red Latosol. Plants were harvested 9 months later, in January 2013 (summer), after an unusually dry winter and spring. Harvest started 2 h before dawn and continued every 2 h until the next dawn (so that each expression time course had 14 time points in total). Dawn was at 5:45, and dusk was at 19:00 (13.25 h light/10.75 h dark) (Fig. S1). At each time point, leaf +1 (the first leaf from the top with clearly visible dewlap), internodes 1 and 2, and internode 5 of nine individuals were harvested (Fig. S2), frozen in liquid N_2, and stored in three pools of three individuals each. Two pools were used as biological replicates for oligoarrays, and one pool was used for validation using the reverse-transcription quantitative PCR (RT-qPCR).

Oligoarray hybridizations

All frozen samples were pulverized in dry ice using a coffee grinder (Model DCG-20, Cuisinart, China). One hundred milligrams of each pulverized sample was used for extraction of total RNA using Trizol (Life Technologies), following the supplier's instructions. The RNA was treated with 2 U DNase I (Life Technologies) for 30 min at 37°C and cleaned using the RNeasy Plant Mini kit (Qiagen). The quality and quantity of RNA were assayed using an Agilent RNA 6000 Nano Kit Bioanalyzer chip (Agilent Technologies). Sample labeling was done following the Low Input Quick Amp Labelling protocol of the Two-Color Microarray-Based Gene Expression Analysis system (Agilent

Technologies). Hybridizations were done using a custom 4×44 k oligoarray (Agilent Technologies) that was previously described (Lembke *et al.*, 2012; Hotta *et al.*, 2013). Two hybridizations were done for each time point against an equimolar pool of all samples of each organ. Each duplicate was prepared independently using dye swaps. Data were extracted using the Feature Extraction software (Agilent Technologies). Background correction was applied to each dataset. A nonlinear LOWESS normalization was also applied to the datasets to minimize variations due to experimental manipulation. Signals that were distinguishable from the local background signal were taken as an indication that the corresponding transcript was expressed. The GenBank ID and Sugarcane Assembled Sequences (SAS) numbers for sugarcane genes are listed in Table S1. The complete dataset can be found at the Gene Expression Omnibus public database under the accession number GSE129543.

Data analysis

For the purposes of further analysis, only transcripts that were found to be expressed in more than 7 of the 14 time points were considered to be expressed. All of the time courses were grouped in coexpressed modules using the R package weighted correlation network analysis (WGCNA) to identify rhythmic transcripts (Langfelder & Horvath, 2008). Network adjacency was calculated using a soft thresholding power of 18 for all organs. Modules that had a dissimilarity value of ≤0.25 were merged. Final modules were generated using a 0.175 adjacency threshold. As WGCNA groups together time courses that have a positive or a negative correlation, we normalized each time course using a *Z*-score, separated these time courses into two new modules, and generated a typical time course for each module by finding the median of all transcripts. Then, each representative time course was classified as rhythmic or nonrhythmic using JTK-CYCLE (Hughes *et al.*, 2010). Modules that had an adjusted *P*-value of <0.75 were considered rhythmic. Finally, we filtered out noisy time courses, defined as those that had a Spearman correlation of <0.3 when compared against the representative time course. Phase was assigned using the phase estimated by JTK-CYCLE corrected against a dendrogram with the representative time courses of all modules of all organs. Modules that clustered together in the dendrogram were considered to have the same phase. The phase of a time course is defined as the time between dawn and the peak of the time course. Euler diagrams were done using the R package *eulerr*. Chi-squared (χ^2) tests were used to compare Euler diagrams. Heatmaps were created using the R packages *circlize* (Gu *et al.*, 2014) and

ComplexHeatmap (Gu *et al.*, 2016). To evaluate if a group of transcripts were under- or overrepresented, we used a hypergeometric test (*phyper* function in R). With this test, a *P*-value < 0.05 suggests that the analyzed group is overrepresented in the dataset, while a *P*-value > 0.95 suggests that the analyzed group is underrepresented in the dataset. Code to fully reproduce our analysis is available on GitHub (https://github.com/LabHotta/sugarcane_field_rhytms) and archived on Zenodo (http://doi.org/10.5281/zenodo.2636813).

RT-qPCR analysis

As described for the oligoarray hybridizations, 100 mg of the pulverized frozen samples for all three organs was used for total RNA extractions following the same Trizol (Life Technologies) protocol and then were treated with DNase I (Life Technologies) and cleansed using the RNeasy Plant Mini Kit (Qiagen). RNA quality and concentration of each sample were checked using an Agilent RNA 6000 Nano Kit Bioanalyzer chip (Agilent Technologies). Five micrograms of total purified RNA was enough for the reverse transcription reactions using the SuperScript III First-Strand Synthesis System for RT-PCR (Life Technologies). The RT-qPCR reactions for all samples were done using Power SYBR Green PCR Master Mix (Applied Biosystems), 10× diluted cDNA, and specific primers described by Hotta et al. (2013) (Figure S8). Reactions were placed in 96-well plates and read with the Fast 7500/7500 Real-Time PCR System (Applied Biosystems). Data analysis was performed using the Fast 7500/7500 Real-Time PCR System built-in software (Applied Biosystems).

Results

A significant proportion of the sugarcane transcriptome is rhythmic in diel conditions

We planted a field of commercial sugarcane (*Saccharum* hybrid SP80-3280) in autumn 2012 in Araras (Brazil, 22°18'41.0"S, 47°23'05.0"W). Nine months later (summer 2013), after a dry winter and spring (Fig. S1), we harvested leaf +1 (L1), internodes 1 and 2 (I1), and internode 5 (I5) every 2 h for 26 h, starting 2 h before dawn. Thus, a time course had 14 time points. On the day of harvest, the stalks were 76 ± 0.16 cm, with 11

219 ± 2 internodes, and their sugar content was 12.0 ± 1.4°Bx (mean ± SD; n = 20). The
220 temperature varied throughout the day from 17°C to 30°C, with the maximum occurring
221 at 11 h after dawn (ZT11); the maximum light intensity was 2.67 MJ/m^2 at ZT07, and
222 dusk occurred 13.25 h after dawn (ZT13.25) (Fig. S1B and D).

223 RNA extracted from each organ was hybridized in 44k custom oligoarrays (Lembke *et*
224 *al.*, 2012; Hotta *et al.*, 2013). Of the 14,521 probes in the array, 12,501 resulted in time
225 courses considered to be expressed in at least one organ (Fig. 1). L1 had 9,822
226 expressed time courses, which was similar to a result obtained in a previous circadian
227 experiment from our group, in which we measured transcripts from 3-month-old leaves
228 (9,932) (Hotta *et al.*, 2013). These datasets shared 94.3% of the expressed time
229 courses (Fig. 1b). I1 had the highest number of expressed time courses (12,053),
230 followed by I5 (10,448). A total of 9,380 time courses were expressed in all three
231 organs (75.0%, Fig. 1e). I1 and I5 shared the most substantial proportion of the time
232 courses considered to be expressed (89.3%), and I1 had the most substantial
233 proportion of unique expressed time courses (7.5%).

234 We identified rhythmic time courses by combining a weighted correlation network
235 analysis (WGCNA) that grouped time courses in coexpression modules (Langfelder &
236 Horvath, 2008) with JTK_CYCLE, which identified which of the modules contained
237 rhythmic time courses (Hughes *et al.*, 2010). This method identified 6,705 rhythmic
238 time courses in L1 (68.3%), 3,755 in I1 (31.2%), and 3,242 in I5 (28.8%) (Fig. 1a and
239 Fig. S3). As a comparison, 32.1% of the time courses were rhythmic in L1 under
240 circadian conditions (Hotta *et al.*, 2013). The overlap between circadian time courses
241 and rhythmic time courses in the field (in diel conditions) was 2,623, representing
242 76.4% of circadian time courses and 60.1% of diel time courses (Fig. 1c).

243

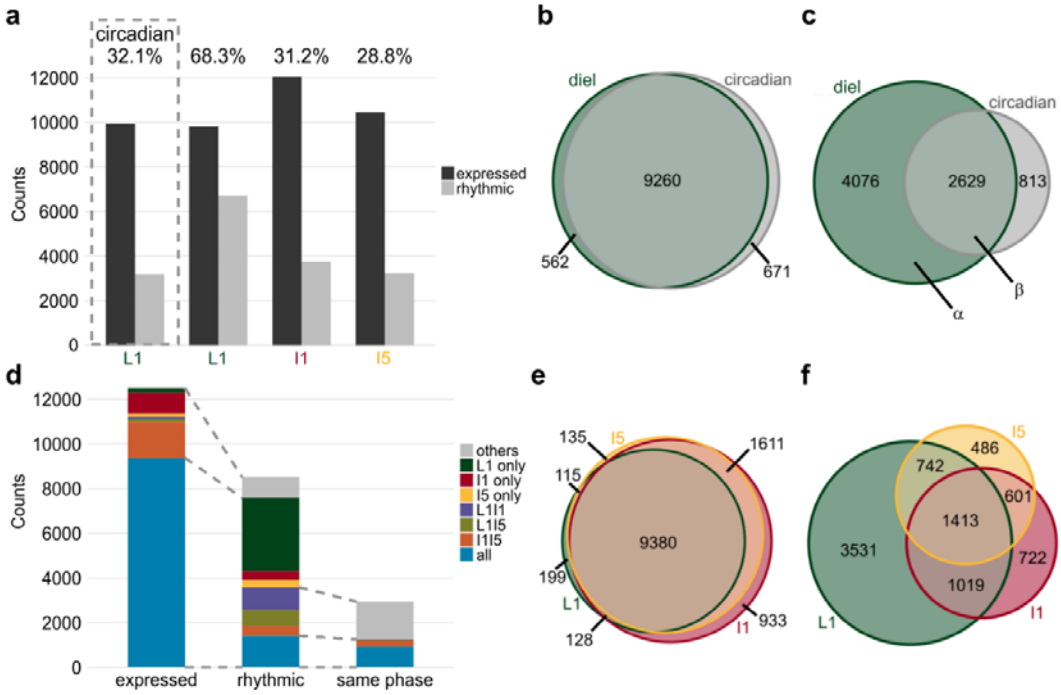

Figure 1 – Different organs have specific sets of rhythmic transcripts in sugarcane. (a) The numbers of expressed and rhythmic time courses detected in leaf +1 (L1), internodes 1 and 2 (I1), and internode 5 (I5) in field-grown (diel) conditions, and in leaf +1 in circadian conditions (Hotta *et al.*, 2013). **(b,c)** Euler diagrams of expressed time courses **(b)** and rhythmic time courses **(c)** in L1 in sugarcane in diel (green) and circadian (gray) conditions. **(d)** Number of expressed time courses, rhythmic time courses, and rhythmic time courses with the same phase that were found specifically in L1, I1, or I5; in both L1 and I1 (L1I1, purple); in both L1 and I5 (L1I5, light green); in both I1 and I5 (I1I5, orange); and in all three organs (L1I1I5, blue). In the second bar, the gray area corresponds to rhythmic time courses that are expressed in only one or two organs. In the third bar, the gray area corresponds to rhythmic time courses in only two organs that have the same phase. The gray dashed lines show the associations among bars. **(e,f)** Euler diagram of expressed and rhythmic time courses in L1, I1, and I5 in field-grown sugarcane in diel conditions.

Different sets of transcripts are rhythmic in different sugarcane organs

Although most expressed time courses were found in all three organs, only 1,413 of the expressed time courses were rhythmic in all three organs (16.6%) (Fig. 1d,f). L1 had the largest proportion of unique rhythmic time courses (41.5%), followed by I1 (8.5%)

and then I5 (5.7%) (Fig. 1f). Time courses that were expressed only in one organ were less likely to be rhythmic (60.3% for L1, 8.6% for I1, and 8.4% for I5) (Fig. 1h).

We estimated the phase of the transcripts by combining the phase calculated using JTK_CYCLE with a dendrogram of the representative time course of each module. Among the time courses that were rhythmic in more than one organ, 27% had rhythms with phase differences >2 h (Fig. 1d). Overall, among the 12,501 unique expressed time courses in the three organs, only 7.4% (923) showed rhythms with the same phase in the three organs. Most of the time courses peaked during the day: this was true of 80.3% in L1, 90.4% in I1, and 96.3% in I5 (the photoperiod was 13.25 h, or 56.3% of a cycle) (Fig. 1g). In L1, 2,363 time courses peaked between dawn (ZT00) and 2 h after dawn (ZT02) (35.2%), and 1,232 time courses peaked at ZT12 (18.4%) (Fig. 2a). When we separated rhythmic L1 time courses into those that were also rhythmic in circadian conditions (Fig. 2b, α) and those that were not (Fig. 2b, β), two different phase distributions could be observed (Fig. 2c). The α group had most time courses peaking at ZT00-02 (39.1%), followed by ZT12 (14.0%), while the β group peaked at ZT12 (25.1%), followed by ZT02 (19.1%). In I1, 1,201 time courses peaked at ZT0 (32.0%) and 716 peaked at ZT8 (19.1%). In I5, 1,373 time courses peaked at ZT0 (42.4%) and 894 peaked at ZT8 (27.6%) (Fig. 2a).

The majority of time courses from L1 (65.8%) grown in diel conditions had the same phase (±2 h) in leaves grown under circadian conditions (Fig. S4a). More time courses showed a delayed peak (19.6%) rather than an advanced peak (13.9%) under diel conditions than under circadian conditions. When we compared L1 and I1 time courses, 65.8% had the same phase, with the remainder divided roughly evenly between delayed and advanced phases (16.1% and 14.9%, respectively) (Fig. S4b). Similarly, 67.1% of the L1 time courses had the same phase as I5, 14.2% had a delayed phase, and 14.8% had an advanced phase (Fig. S4c). The phases were most similar between I1 and I5 time courses: 93.8% had the same phases, 2.8% a phase delay, and 3.1% a phase advance (Fig. S4d).

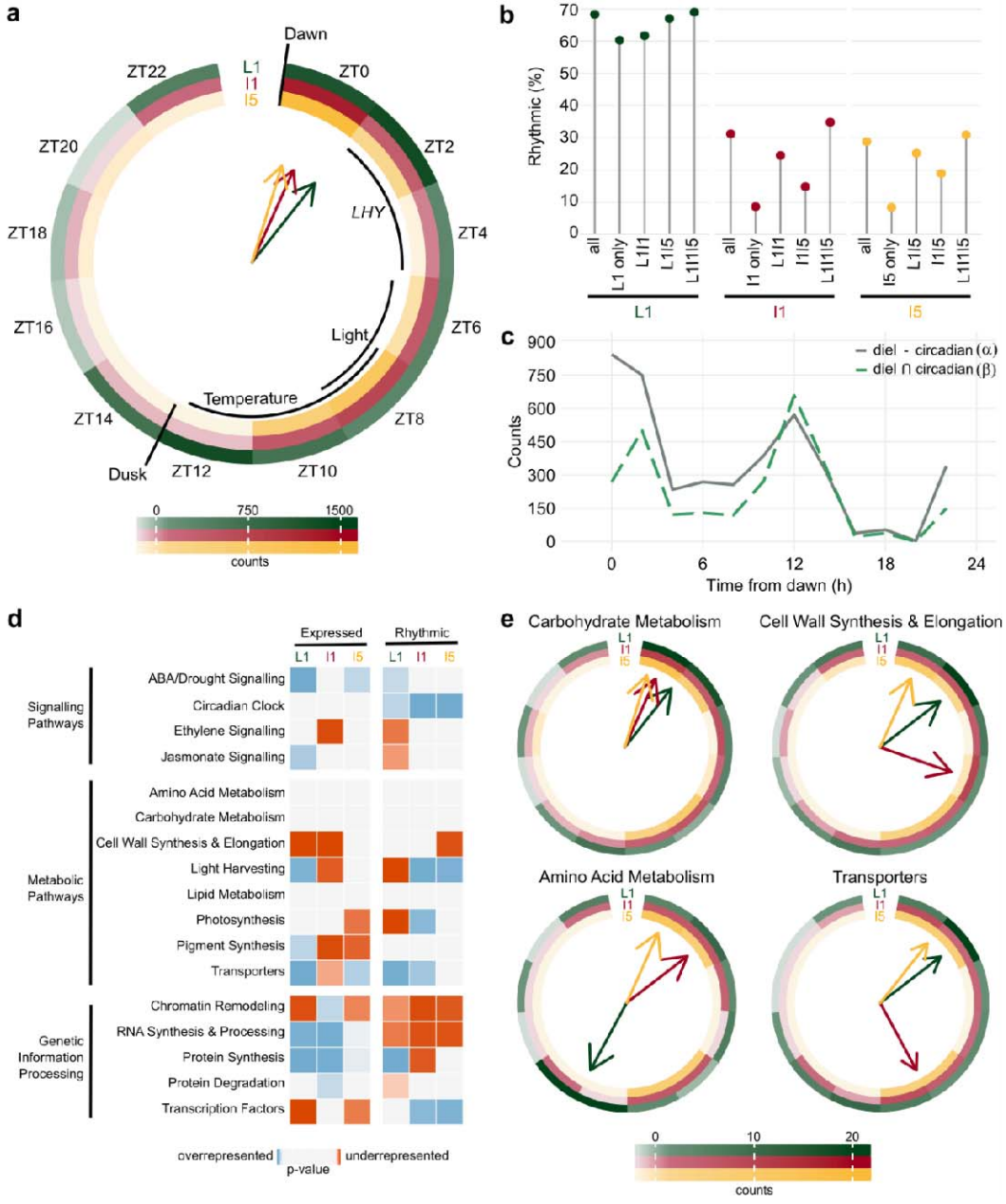

Figure 2 – Transcripts have unique phases in different sugarcane organs. (a) Circular heatmap of the rhythmic transcript peak time (ZT0 = 0 h after dawn) distribution in leaf +1 (L1), internodes 1 and 2 (I1), and internode 5 (I5). The colored arrows show the times at which the most transcripts are found in each organ. The times of dawn, dusk, *LHY* transcription peak, maximum light intensity, and maximum temperatures are indicated by black arcs. **(b)** Proportions of transcripts that were rhythmic in L1, I1, and I5 among all expressed transcripts in each organ (All), among the transcripts expressed only in one organ (L1 only, I1 only, or I5 only), among the transcripts expressed in two organs (L1I1, L1I5, or I1I5), and among transcripts

expressed in all three organs (L1I1I5). **(c)** Distribution of rhythmic transcript peak time in time courses that were rhythmic in L1 but not in circadian conditions (α in Fig. 1c) and rhythmic transcripts in time courses that were rhythmic in L1 and circadian conditions (β). **(d)** Heatmap of functional categories that are overrepresented (shades of blue) or underrepresented (shades of red) among the expressed and rhythmic transcripts of L1, I1, and I5. The *P*-value was calculated using a hypergeometric test. **(e)** Circular heatmap with the distribution of the peak times of rhythmic transcripts associated with the pathways *Carbohydrate Metabolism*, *Cell Wall Synthesis & Elongation*, *Amino Acid Metabolism*, and *Transporters*.

Biochemical pathways have different rhythms in sugarcane organs

We used a hypergeometric test to detect if a pathway was over- or underrepresented by comparing the frequency of transcripts associated with a Biochemical Pathway among the expressed time courses and all the unique transcripts in the oligoarray (Fig. 2d and Fig. S5). We used the same test comparing the frequency of transcripts associated with a Biochemical Pathway among the rhythmic time courses and the expressed time courses (Fig. 2d and Fig. S5). The transcript annotations were based on the SUCEST database annotation (http://sucest-fun.org).

Among expressed time courses, each organ has a distinct profile. For example, L1 was the only organ that had the *Pigment Synthesis*, *Light Harvesting*, and *Jasmonate Signaling* pathways considered to be overrepresented. I1 had *Chromatin Remodeling* and *Protein Synthesis* pathways overrepresented and *Ethylene Signaling* underrepresented. *Transcription Factors* was underrepresented and *ABA/Drought Signaling* and *Transporters* were overrepresented in L1 and I5, but not in I1. I5 is the only organ in which *Cell Wall Synthesis & Elongation* was not underrepresented among the expressed time courses (Fig. 2d). Among rhythmic time courses, *Circadian Clock* was overrepresented, while *Chromatin Remodeling* and *RNA Synthesis & Processing* were underrepresented in all organs. *Protein Synthesis* was overrepresented in L1. *Transcription Factors* was overrepresented in I1 and I5, and *Transporters* was overrepresented among rhythmic time courses in L1 and I1 (Fig. 2d).

When we analyzed time courses associated with important pathways for sugarcane growth, we found further organ-specific patterns; these differences could be seen in both expressed and rhythmic time courses, as well as the phase of the rhythmic time courses (Fig. 2e and Fig. S6). Time courses associated with *Carbohydrate Metabolism*

tended to peak in the morning. Almost half (48.0%) of the time courses had a peak at ZT00 in L1, while the majority peaked between ZT00 and ZT04 in both I1 (53.2%) and I5 (58%) (Fig. 2e). Amongst the individual time courses, a putative ortholog of *SUCROSE SYNTHASE4* (*SuSy4*) had a similar rhythmic pattern in all three organs. A putative ortholog of *SUCROSE-PHOSPHATE SYNTHASE II* (*SPSII*) was rhythmic only in L1, while a putative ortholog of a *CELL WALL INVERTASE* (*CWI*) exhibited a sharp peak at ZT04 in L1 but a very broad peak at ZT08 in I1 and I5 (Fig. 6i, m and q).

Time courses associated with *Cell Wall Synthesis & Elongation* had a more diverse phase distribution: in L1, 55% had a peak between ZT00 and ZT04 in L1; in I1, 73.4% had a peak between ZT00 and ZT08; and in I5, 45.8% had a peak between ZT08 and ZT10 and 37.8% had one at ZT00 (Fig. 2e). There was also a higher proportion of time courses associated with *Cell Wall Synthesis & Elongation* that are expressed only in I1 and I5 (Fig. S6). Time courses associated with *Amino Acid Metabolism* peaked between ZT12 and ZT14 in L1 (50%). In I1 and I5, they had two peaks: between ZT00 and ZT02 (37.5% and 57.1%) and between ZT08 and ZT10 (37.5% and 42.9%) (Fig. 2b). Time courses associated with *Transporters* peaked at ZT02 (35.7%) and ZT12 (15.7%) in L1. In I1, most of the time courses peaked 2 h earlier, at ZT00 (24.2%) and ZT10 (24.2%). I5 displayed a similar pattern to I1, with 53.6% peaking between ZT00 and ZT02 and 46.4% between ZT08 and ZT10 (Fig. 2b). This tendency for L1 to have later phases than I1 and I5 can be seen in the putative ortholog *SWEET2*, which peaked at ZT02 in L1 and at ZT18-20 in I1 and I5 (Fig. 6l).

Circadian clock transcripts have similar dynamics in different sugarcane organs

The differences in the rhythmic time courses of the three organs could be explained by the presence of organ-specific circadian clocks that could generate different patterns of rhythmic transcription. The circadian clocks can be divided into three parts: *Input Pathways*, *Central Oscillator*, and *Output Pathways* (Henriques *et al.*, 2018).

Most of the known *Input Pathways* to the circadian clock are associated with *Light Signaling* (Oakenfull & Davis, 2017). *Light Signaling* is underrepresented among the transcripts expressed in I5 and the rhythmic time courses in I1 (Fig. S5). Among the red light receptor genes, *PHYTOCHROME A.1* (*PHYA.*1) was rhythmic in L1, with a peak at ZT23, while *PHYB* was not rhythmic in any organ (Fig. S7a,b). In I1 and I5, both *PHYs* had two peaks: one near dawn (ZT00-02) and another at night (ZT18-20). Among the blue light receptors, *CRYPTOCHROME1.1* (*CRY1.1*) was rhythmic in L1,

371 peaking at ZT03. *CRY2.1* was rhythmic in I5, peaking at ZT19. *ZEITLUPE* (*ZTL.1*) was
372 rhythmic in L1 and I5, peaking at ZT01 and ZT21, respectively (Fig. S7d-f).

373 The *Central Oscillator* generates rhythms that can run independently from
374 environmental rhythms. In general, the time courses associated with the *Central*
375 *Oscillator* displayed rhythms with similar dynamics (Fig. 3). *LHY* peaked early in the
376 morning, between ZT02 and ZT04, with overlapping dynamics in all three organs (Fig.
377 3a). Similarly, *TOC1* peaked around dusk, between ZT10 and ZT12, in all three organs
378 (Fig. 3d). The normalizations used to analyze the oligoarray data do not allow the
379 comparison of expression levels, so we used RT-qPCR to show that *LHY* varied during
380 the day by 750× in L1 and 150× in I1 and I5 (Fig. S8a). In contrast, *TOC1* differed 30×
381 in L1 and 18× in I1 and I5 (Fig. S8b). The other PRR genes, *PRR59*, *PRR73*, and
382 *PRR95* (referred to as *ScPRR3*, *ScPRR7*, and *ScPRR59*, respectively, in Hotta *et al.*,
383 2011), peaked between ZT06 and ZT10 (Fig. 3b, c, and e). *GI* peaked between ZT08
384 and ZT10 in all three organs (Fig. 3f). Finally, *ELF3* was rhythmic only in L1, with a
385 peak at ZT14. In the internodes, *ELF3* had a similar pattern, but it was not regarded as
386 rhythmic due to high noise (Fig. S7c).

387 Among the possible pathways that can be recruited by the circadian clock that are
388 considered part of the *Output Pathways* are those associated with *Chromatin*
389 *Remodeling*, *Transcription Factors*, and *Protein Synthesis* (Fig. 4). Time courses
390 associated with *Chromatin Remodeling* peaked at ZT00-02 and ZT10-12 in L1 (32.5%
391 and 36.5%, respectively). In I1 and I5, they peaked at ZT00 (40.7% and 40.8%,
392 respectively) and ZT08-10 (33.99% and 51.2%, respectively) (Fig. 4a). Time courses
393 associated with *Transcription Factors* tended to peak near dawn, at ZT00-02, in all
394 three organs (57.5% in L1, 46.4% in i1, and 50.3% in I5). A higher proportion (22.6%)
395 of time courses associated with *Transcription Factors* were rhythmic when compared to
396 all rhythmic (16.6%) time courses, $\chi^2(6, n = 341) = 15.1$, $P = 0.02$ (chi-square test, Fig.
397 4e). These time courses also peaked similarly in all organs: 79.3% peaked in the same
398 interval in L1 as in I1, 72.2% peaked in the same interval in L1 and I5, and 93.1% in I1
399 and I5.

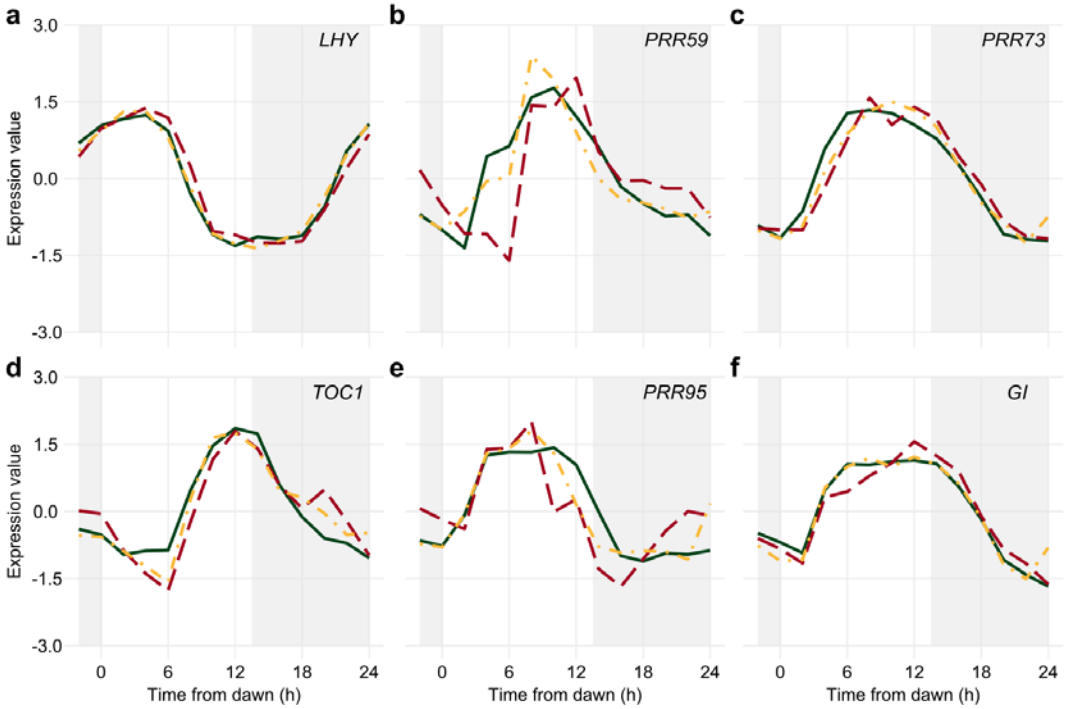

Figure 3 – Diel rhythms of *Central Oscillator* transcripts in sugarcane organs. *LHY* **(a)**, *PRR59* **(b)**, *PRR73* **(c)**, *TOC1* **(d)**, *PRR95* **(e)**, and *GI* **(f)** rhythms were measured in leaf +1 (L1, green continuous line), internodes 1 and 2 (I1, red dashed line), and internode 5 (I5, yellow dash-dotted line) of field-grown sugarcane using oligoarrays. Time courses were normalized using *Z*-score. The light-gray boxes represent the night periods.

Time courses associated with *Protein Synthesis* tended to peak at dusk in L1 (ZT12, 49.0%), at dawn and afternoon in I1 (ZT00, 36.1%; ZT10, 32.5%), and at dawn in I5 (ZT00, 61.7%) (Fig. 4c). A higher proportion of time courses associated with *Protein Synthesis* were expressed in all three organs (91.4%) than for all time courses (75.0%), $\chi^2(6, n = 314) = 48.7$, $P < 0.001$ (Fig. 4f). In contrast, more than half of the time courses (54.6%) were rhythmic only in L1, whereas a lower frequency (41.5%) of total rhythmic time courses were seen only in L1, $\chi^2(6, n = 269) = 34.8$, $P < 0.001$ (Fig. 4i).

Other time courses showed a wide variety of oscillations amongst the three organs (Fig. 4j-l, and S9). The putative *STRUCTURAL MAINTENANCE OF CHROMOSOMES1* (*SMC1*), associated with *Chromatin Remodeling*, peaked at ZT06 in L1 and ZT11 in I1 and I5 (Fig. 4j). Two putative *JUMONJI-C (JMJC) DOMAIN-CONTAINING PROTEIN5* (*JMJD5*) genes, encoding proteins that can act as histone

demethylases, were found in sugarcane. *JMJD5.1* is expressed only in I1 and I5 and has a phase at ZT10 (Fig. S9a,d); *JMJD5.2* is expressed in all organs with similar rhythmic patterns (Fig. S9a). The transcription factor gene *HOMEOBOX PROTEIN24* (*HB24*) is rhythmic only in L1, with a peak at ZT10 (Fig. 4k). Another rhythmic gene, *40S RIBOSOMAL PROTEIN S15* (*S15A*), associated with *Protein Synthesis*, has a peak at ZT14 in L1 and at ZT00 in I1 and I5 (Fig. 4l).

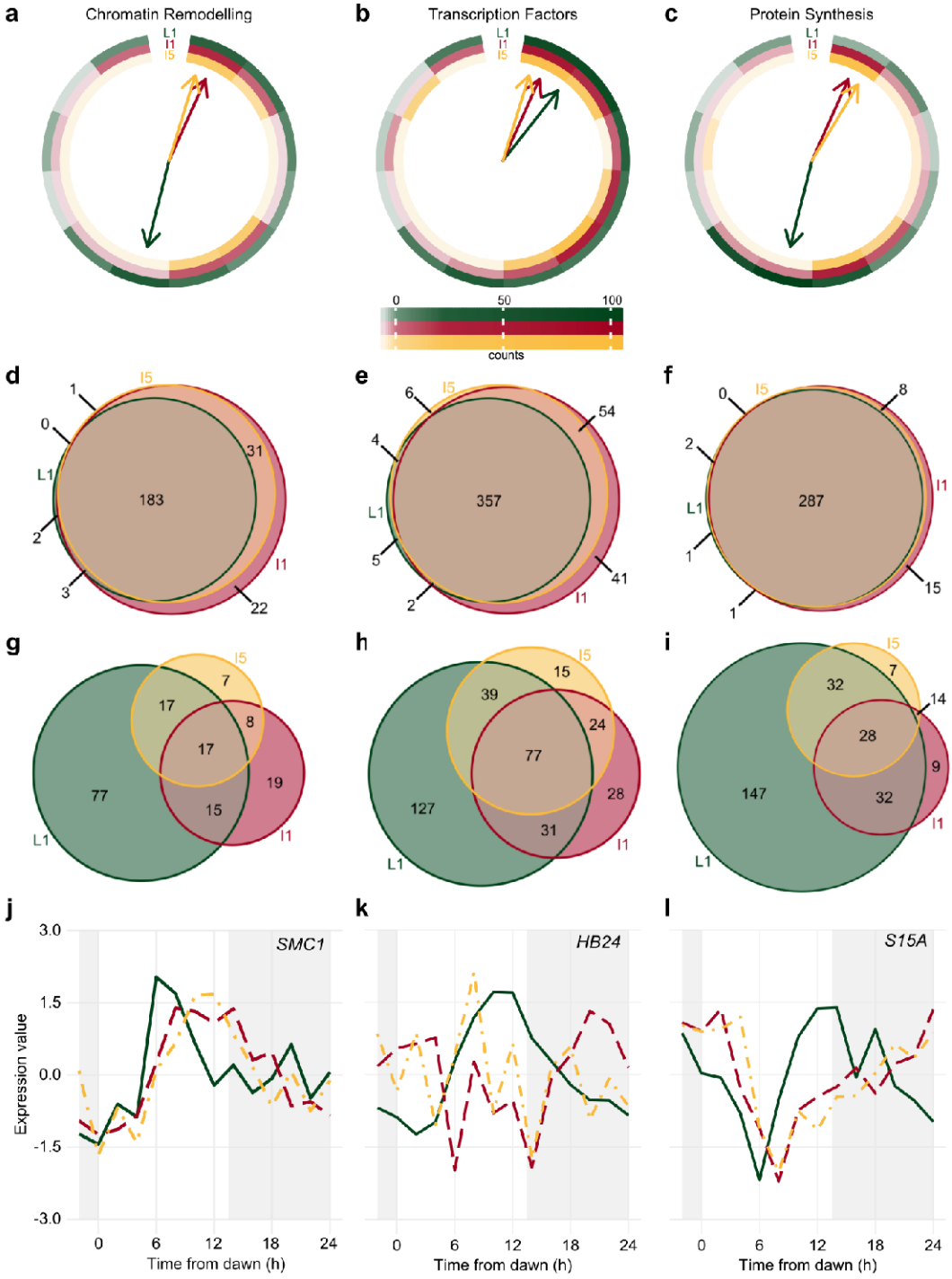

Figure 4 – Transcripts associated with *Genetic Information Processing* have different rhythms in sugarcane organs. (a-c) Circular heatmap of the distribution of the peak time of rhythmic transcripts related to *Chromatin Remodeling* **(a)**, *Transcription Factors* **(b)**, and *Protein Synthesis* **(c)** in leaf +1 (L1, green), internodes 1 and 2 (I1, red), and internode 5 (I5, yellow). The colored arrows show the time at which the most transcripts are found in each organ. **(d-i)** Euler diagrams of all expressed transcripts **(d-f)** and rhythmic transcripts **(g-i)** in L1, I1, and I5 in field-grown sugarcane in diel conditions. **(j-l)** *SMC1* **(j)**, *HB24* **(k)**, and *S15A* **(l)** rhythms measured in L1 (continuous green line), I1 (red dashed line), and I5 (yellow dash-dotted line) of field-grown sugarcane using oligoarrays. Time courses were normalized using *Z*-score. The light-gray boxes represent the night periods.

Discussion

Organ-specific rhythms of transcription can be found in highly productive and intensively selected commercial sugarcane. The specialization of the rhythmic transcriptome may help the plant cells to adapt to local environmental rhythms, as well as to generate rhythms that are compatible with their specialized needs. Specialized rhythms may also be essential to rhythmic processes that require organ-to-organ coordination, such as sucrose transport from the leaves to the internodes (Wang *et al.*, 2013).

Rhythms in field conditions are different from those in controlled conditions

Sugarcane leaves in field conditions had twice as many time courses identified as rhythmic than plants assayed under circadian conditions. This difference is expected because some rhythms are driven by environmental oscillations, such as light and temperature. Also, some circadian-clock-driven rhythms may undergo amplitude increases due to a general increase in the amplitude of the *Central Oscillator*. In L1, the transcriptional rhythms of *LHY* vary by up to 60× in a day in circadian conditions and 750× in field conditions, while those of *TOC1* vary up to 5× in a day in circadian conditions and 40× in field conditions (Hotta et al., 2013, and Fig. S8). In circadian conditions, most time courses peaked at subjective dusk (ZT12, 29.0%), which resulted in 60.5% of the time courses peaking during subjective night.

By contrast, in field conditions, most time courses peaked near dawn (ZT00-02, 35.2%) in L1, which resulted in 80.3% of the time courses peaking during the day. This reinforces the role of the light/dark transition as the driving force of rhythms in leaves in field conditions. A high proportion (64.1%) of the time courses that peaked during the subjective night in circadian conditions showed phase changes that resulted in higher expression during the day in field conditions. This might suggest the existence of dampening mechanisms that actively decrease nocturnal peaks. A similar mechanism keeps cytoplasmic calcium concentration lower during the night under diel conditions (day/night) than during the subjective night under circadian conditions (Xu *et al.*, 2007). Most of the time courses associated with the *Central Oscillator* maintained their core phases, except *LHY*, which had a later peak (ZT01 in circadian conditions; ZT04 in field conditions). As a comparison, *LHY* is induced by light in Arabidopsis and is mostly insensitive to temperature in rice (Kim *et al.*, 2003; Nagano *et al.*, 2012). The differences between the rhythmic transcriptomes in circadian conditions and field conditions highlight the importance of experiments done under field conditions to understanding how the circadian clock can affect the plant transcriptome *in natura*.

Rhythmic transcripts are organ-specific

The time courses in L1, I1, and I5 have very different rhythmic patterns, even though most of the expressed time courses were found in all three organs. Rhythms in I1 and I5 were more similar to each other than to those in L1, and only 7.4% of the time courses expressed in all three organs showed the same rhythms. Thus, we conclude that these three organs have vastly different and specialized circadian clocks. These specialized circadian clocks could be the result of multiple organ sensitivities to environmental cues, of organ-specific *Core Oscillators*, and of organ-specific interactions of *Output Pathways* with environmental signals.

In Arabidopsis, different sensitivities to environmental cues are found in the vascular phloem companion cells, which are more sensitive to photoperiodism, and the epidermis cells, which are more sensitive to temperature (Shimizu *et al.*, 2015). In sugarcane, most L1 time courses peak at ZT00-02 and ZT12, following dawn and dusk, while most I1 and I5 time courses peak at ZT00 and ZT08, following dawn and the daily light and temperature maxima. Thus, the circadian clocks of these organs respond differently to environmental cues such as photoperiod, light/dark transition, or temperature, as in Arabidopsis. In rice, a significant proportion of rhythmic transcripts are regulated either by the circadian clock or by temperature oscillations (Nagano *et*

494 *al.*, 2012). In sugarcane, rhythmic L1 time courses that were also rhythmic in circadian
495 conditions had peaks that follow *LHY* or *TOC1* expression. On the other hand, rhythmic
496 L1 time courses that were not rhythmic in circadian conditions peaked at dawn and
497 dusk. In internodes, time courses peaked at dawn and at the light and temperature
498 maximum. Such organ-specific sensitivity to environmental cues was previously
499 described in the vasculature and epidermis (Shimizu *et al.*, 2015).

500 The *Central Oscillators* of mesophyll and vasculature in Arabidopsis have similar
501 components but with different amplitudes. *AtELF4* rhythms have an amplitude 10×
502 higher in the vasculature, *AtPRR7* and *AtPRR9* amplitudes are 2× higher in the
503 mesophyll, and *AtTOC1* amplitude is similar in both tissues (Endo *et al.*, 2014). In
504 sugarcane, *LHY* amplitude is 6× higher and *TOC1* amplitude is 2× higher in L1
505 compared to I1 and I5. As leaves are exposed to direct sunlight, whereas internodes
506 are protected by layers of leaf sheaths, it is probable that sunlight is responsible for
507 these amplitude differences. The dynamics of *LHY*, *TOC1*, and *GI* during the day were
508 very similar in the three organs. Indeed, they were considered to be coexpressed when
509 analyzed together (data not shown). As the three organs have different levels of
510 exposure to the environment, the existence of a common environmental signal is
511 unlikely. Alternatively, the oscillators of the three organs could be coupled. There is
512 evidence in Arabidopsis of root oscillators being regulated by the oscillators of the
513 aerial parts of the plants, either the leaves or the shoot apical meristem (SAM) (James
514 *et al.*, 2008; Takahashi *et al.*, 2015). As the leaves are a source signal to both
515 internodes, it is possible that synchronizing signals are transported with sucrose and
516 other sugars. In Arabidopsis, sugars can also act as an entrainment signal (Haydon *et*
517 *al.*, 2013; Frank *et al.*, 2018).

518 Even though there is much evidence for tissue-specific circadian clocks in Arabidopsis
519 (Para *et al.*, 2007; Xu *et al.*, 2007; Kim *et al.*, 2011; Endo *et al.*, 2014; Endo, 2015), less
520 is known about their effect on the rhythmic regulation of transcripts. In contrast, tissue-
521 specific rhythms have been widely studied in mammals (Storch *et al.*, 2002; Panda *et*
522 *al.*, 2002; Zhang *et al.*, 2014; Ruben *et al.*, 2018). Sampling of 12 different mouse
523 organs over time showed that 43% (~8,500) of all transcripts had circadian rhythms in
524 at least one organ, but only 10 transcripts were rhythmic in all organs (Zhang *et al.*,
525 2014). As in sugarcane leaves, the rhythmic transcripts in mammalian organs tended to
526 peak at dawn and dusk. In general, the only transcripts that had similar phases across
527 all organs were the ones associated with the mammalian *Core Oscillato*r (Zhang *et al.*,
528 2014).

529 At least two regulatory pathways are required to generate tissue-specific sets of
530 rhythmic transcripts: one that confers organ specificity and one that confers rhythmicity.
531 These pathways can be organized in different nonexclusive ways: they could act on a
532 gene independently, the tissue specificity pathways could regulate the rhythmicity
533 pathways, or the rhythmicity pathways could regulate the organ specificity pathways
534 (Fig. S10). The rhythmicity pathways can be dependent on the circadian clock, on
535 environmental rhythms, or both. The tissue specificity pathways can include
536 transcription factors, protein-protein interactions, alternative promoter usage, chromatin
537 interactions, and topologically associating domains (TADs) (Yeung & Naef, 2018).

538 In our datasets, time courses that were expressed only in one organ or only in the
539 internodes were less likely to be considered rhythmic (Fig. 2b). Thus, it is possible that
540 rhythmic pathways regulate only a small proportion of organ-specific pathways. Time
541 courses associated with *Transcription Factors* were more likely to be rhythmic in all
542 three organs, and these time courses had a higher probability of having the same
543 phase. However, just a few tissue-specific rhythms in transcription factors can have a
544 sizeable cascading effect (Yeung *et al.*, 2018). Tissue-specific transcription factors,
545 even if nonrhythmic, could also change the phase of rhythmic transcripts through
546 protein-protein interactions or by changing the promoter usage (Smieszek *et al.*, 2014;
547 Yeung & Naef, 2018). Finally, chromatin remodeling could be a significant regulatory
548 pathway in the generation of the tissue-specific rhythmic transcriptome. In Arabidopsis,
549 chromatin remodeling can regulate the *Central Oscillator*, but little is known about how
550 the plant circadian clock can use chromatin remodeling to generate rhythms (Lu *et al.*,
551 2011; Malapeira *et al.*, 2012; Lee *et al.*, 2015; Yang *et al.*, 2018). In sugarcane,
552 rhythms in time courses associated with *Chromatin Remodeling* were
553 underrepresented among the rhythmic time courses. However, chromatin remodeling
554 tends to be regulated post-transcriptionally through histone modifications. Transcription
555 can also be regulated at the chromatin level through TADs. In mammals, TADs can be
556 regulated to generate tissue-specific transcription and even rhythms (Aguilar-Arnal *et*
557 *al.*, 2013; Kim *et al.*, 2018; Mermet *et al.*, 2018). In plants, TADs are maintained by
558 cohesins, but there are still no known CCCTC-binding factors (CTCF) counterparts
559 (Schubert *et al.*, 2013; Liu *et al.*, 2017). In sugarcane, the cohesin subunit *SMC1* has
560 different phases in leaves and internodes.

561 Specialized tissue-specific circadian clocks allow the different tissues to be more
562 efficient according to their function and local environmental rhythms (Yeung & Naef,
563 2018). In mammals, rhythms in fibroblasts allow wound healing to occur faster during
564 the active phase than the rest phase (Hoyle *et al.*, 2017). Furthermore, rhythms in the

565 liver lead to larger cell sizes and protein levels during the active phase and after
566 feeding, making detoxification more efficient during the active and post-feeding periods
567 (Sinturel *et al.*, 2017). In sugarcane, expressed time courses associated with
568 *Transporters* were overrepresented in L1 and I5, while rhythmic time courses
569 associated with *Transporters* were overrepresented in L1 and I1. Nutrient and
570 photosynthate transportation inside the plant are essential for rhythmic processes and
571 may also be part of organ-to-organ coordination (Wang *et al.*, 2013; Xu, 2018; López-
572 Salmerón *et al.*, 2019). Sucrose accumulation in the internodes inhibits leaf
573 photosynthesis in sugarcane (Ribeiro *et al.*, 2017). Furthermore, time courses
574 associated with *Transporters* tended to peak 2 h later in L1 than in the internodes,
575 which may indicate that the latter is the driving force of this process. Other processes,
576 such as *Pigment Synthesis* and *Light Harvesting* in L1, *Chromatin Remodeling* and
577 *Protein Synthesis* in I1, and *Cell Wall Synthesis & Elongation* in I5, also suggest a
578 functional specialization to the organ-specific circadian clock.

579 The vast differences found in the rhythmic transcriptomes of different plant organs
580 provide important clues to understanding the way that tissue-specific circadian clocks
581 are generated and their impact on plant physiology. However, little is still known about
582 the molecular mechanisms that control this specialization. The combination of organ- or
583 tissue-specific studies with the observation of rhythms in the field, where conditions are
584 fluctuating and variable as is normal in natural environments, is essential to
585 understanding the nuances of how the plant circadian clock increases the fitness of
586 plants and, in turn, crop productivity.

587

588 **Acknowledgments**

589 This work was supported by the São Paulo Research Foundation (FAPESP) (grant
590 nos. 11/00818-8 and 15/06260-0; BIOEN Program) and by the Serrapilheira Institute
591 (grant no. Serra-1708-16001). L.L.B.D, C. A. L., and N. O. L. were supported by
592 FAPESP scholarships (grants 11/08897-4, 13/05301-9, and 16/06740-4, respectively).

593

594 **Author Contributions**

595 Conceptualization, L.L.B.D., M.S.C., G.M.S., C.T.H; Methodology, L.L.B.D., C.T.H;
596 Software, M.Y.N., C.T.H; Validation, L.L.B.D., N.O.L.; Investigation, L.L.B.D., N.O.L.,
597 C.A.L., C.T.H; Resources, M.S.C., G.M.S.; Data Curation, M.Y.N., C.T.H; Writing –

598 Original Draft, L.L.B.D., C.T.H; Writing – Review & Editing, L.L.B.D., C.A.L., C.T.H;
599 Visualization; C. T. H.; Project Administration, C. T. H.; Funding Acquisition, C.T.H

600

601 ## References

602 **Aguilar-Arnal L, Hakim O, Patel VR, Baldi P, Hager GL, Sassone-Corsi P. 2013**. Cycles in spatial
603 and temporal chromosomal organization driven by the circadian clock. *Nature Structural &*
604 *Molecular Biology* **20**: 1206–1213.

605 **Annunziata MG, Apelt F, Carillo P, Krause U, Feil R, Koehl K, Lunn JE, Stitt M. 2018**. Response
606 of Arabidopsis primary metabolism and circadian clock to low night temperature in a natural
607 light environment. *Journal of Experimental Botany* **69**: 4881–4895.

608 **Calixto CPG, Waugh R, Brown JWS. 2015**. Evolutionary relationships among barley and
609 Arabidopsis core circadian clock and clock-associated genes. *Journal of Molecular Evolution* **80**:
610 108–119.

611 **Dodd AN, Salathia N, Hall A, Kevei E, Toth R, Nagy F, Hibberd JM, Millar AJ, Webb AA. 2005**.
612 Plant circadian clocks increase photosynthesis, growth, survival, and competitive advantage.
613 *Science* **309**: 630–3.

614 **Endo M. 2015**. Tissue-specific circadian clocks in plants. *Current Opinion in Plant Biology* **29**:
615 44–49.

616 **Endo M, Shimizu H, Nohales MA, Araki T, Kay SA. 2014**. Tissue-specific clocks in Arabidopsis
617 show asymmetric coupling. *Nature* **515**: 419–22.

618 **Frank A, Matiolli CC, Viana AJC, Hearn TJ, Kusakina J, Belbin FE, Wells Newman D, Yochikawa**
619 **A, Cano-Ramirez DL, Chembath A, *et al.* 2018**. Circadian entrainment in Arabidopsis by the
620 sugar-responsive transcription factor bZIP63. *Current Biology* **28**: 2597-2606.e6.

621 **Gawroński P, Ariyadasa R, Himmelbach A, Poursarebani N, Kilian B, Stein N, Steuernagel B,**
622 **Hensel G, Kumlehn J, Sehgal SK, *et al.* 2014**. A distorted circadian clock causes early flowering
623 and temperature-dependent variation in spike development in the Eps-3Am mutant of einkorn
624 wheat. *Genetics* **196**: 1253–1261.

625 **Glassop D, Rae AL. 2019**. Expression of sugarcane genes associated with perception of
626 photoperiod and floral induction reveals cycling over a 24-hour period. *Functional Plant*
627 *Biology* **46**: 314–327.

628 **Green RM, Tingay S, Wang Z-Y, Tobin EM. 2002**. Circadian rhythms confer a higher level of
629 fitness to Arabidopsis plants. *Plant Physiology* **129**: 576–584.

630 **Gu Z, Eils R, Schlesner M. 2016**. Complex heatmaps reveal patterns and correlations in
631 multidimensional genomic data. *Bioinformatics* **32**: 2847–2849.

632 **Gu Z, Gu L, Eils R, Schlesner M, Brors B. 2014**. circlize Implements and enhances circular
633 visualization in R. *Bioinformatics (Oxford, England)* **30**: 2811–2812.

Haydon MJ, Mielczarek O, Robertson FC, Hubbard KE, Webb AA. **2013**. Photosynthetic entrainment of the Arabidopsis thaliana circadian clock. *Nature* **502**: 689–92.

Henriques R, Papdi C, Ahmad Z, Bögre L. **2018**. Circadian regulation of plant growth. In: Annual Plant Reviews online. American Cancer Society, 1–29.

Hotta CT, Gardner MJ, Hubbard KE, Baek SJ, Dalchau N, Suhita D, Dodd AN, Webb AA. **2007**. Modulation of environmental responses of plants by circadian clocks. *Plant Cell Environ* **30**: 333–49.

Hotta CT, Nishiyama MY, Souza GM. **2013**. Circadian rhythms of sense and antisense transcription in sugarcane, a highly polyploid crop. *PLoS One* **8**: e71847.

Hoyle NP, Seinkmane E, Putker M, Feeney KA, Krogager TP, Chesham JE, Bray LK, Thomas JM, Dunn K, Blaikley J, *et al.* 2017. Circadian actin dynamics drive rhythmic fibroblast mobilization during wound healing. *Science Translational Medicine* **9**.

Hsu PY, Devisetty UK, Harmer SL. **2013**. Accurate timekeeping is controlled by a cycling activator in Arabidopsis. *eLife* **2**: e00473.

Hughes ME, Hogenesch JB, Kornacker K. **2010**. JTK_CYCLE: an efficient nonparametric algorithm for detecting rhythmic components in genome-scale data sets. *Journal of Biological Rhythms* **25**: 372–380.

Izawa T, Mihara M, Suzuki Y, Gupta M, Itoh H, Nagano AJ, Motoyama R, Sawada Y, Yano M, Hirai MY, *et al.* 2011. Os-GIGANTEA confers robust diurnal rhythms on the global transcriptome of rice in the field. *The Plant Cell* **23**: 1741–1755.

James AB, Monreal JA, Nimmo GA, Kelly CL, Herzyk P, Jenkins GI, Nimmo HG. **2008**. The circadian clock in Arabidopsis roots is a simplified slave version of the clock in shoots. *Science* **322**: 1832–5.

Kim YH, Marhon SA, Zhang Y, Steger DJ, Won K-J, Lazar MA. **2018**. Rev-erbα dynamically modulates chromatin looping to control circadian gene transcription. *Science (New York, N.Y.)* **359**: 1274–1277.

Kim J-Y, Song H-R, Taylor BL, Carré IA. **2003**. Light-regulated translation mediates gated induction of the Arabidopsis clock protein LHY. *The EMBO Journal* **22**: 935–944.

Kim S-G, Yon F, Gaquerel E, Gulati J, Baldwin IT. **2011**. Tissue specific diurnal rhythms of metabolites and their regulation during herbivore attack in a native tobacco, Nicotiana attenuata. *PloS One* **6**: e26214.

Kusakina J, Rutterford Z, Cotter S, Martí MC, Laurie DA, Greenland AJ, Hall A, Webb AAR. **2015**. Barley Hv CIRCADIAN CLOCK ASSOCIATED 1 and Hv PHOTOPERIOD H1 are circadian regulators that can affect circadian rhythms in Arabidopsis. *PloS One* **10**: e0127449.

Langfelder P, Horvath S. **2008**. WGCNA: an R package for weighted correlation network analysis. *BMC bioinformatics* **9**: 559.

Lee HG, Lee K, Jang K, Seo PJ. **2015**. Circadian expression profiles of chromatin ing factor genes in Arabidopsis. *Journal of Plant Research* **128**: 187–199.

672 **Lembke CG, Nishiyama MY, Sato PM, de Andrade RF, Souza GM**. **2012**. Identification of sense
673 and antisense transcripts regulated by drought in sugarcane. *Plant Molecular Biology* **79**: 461–
674 477.

675 **Liu C, Cheng Y-J, Wang J-W, Weigel D**. **2017**. Prominent topologically associated domains
676 differentiate global chromatin packing in rice from Arabidopsis. *Nature Plants* **3**: 742–748.

677 **López-Salmerón V, Cho H, Tonn N, Greb T**. **2019**. The phloem as a mediator of plant growth
678 plasticity. *Current biology: CB* **29**: R173–R181.

679 **Lu SX, Knowles SM, Webb CJ, Celaya RB, Cha C, Siu JP, Tobin EM**. **2011**. The Jumonji C
680 Domain-Containing Protein JMJ30 regulates period length in the Arabidopsis circadian clock.
681 *Plant Physiology* **155**: 906–915.

682 **Malapeira J, Khaitova LC, Mas P**. **2012**. Ordered changes in histone modifications at the core
683 of the Arabidopsis circadian clock. *Proc Natl Acad Sci U S A* **109**: 21540–5.

684 **Matsuzaki J, Kawahara Y, Izawa T**. **2015**. Punctual transcriptional regulation by the rice
685 circadian clock under fluctuating field conditions. *The Plant Cell* **27**: 633–648.

686 **Mermet J, Yeung J, Hurni C, Mauvoisin D, Gustafson K, Jouffe C, Nicolas D, Emmenegger Y,**
687 **Gobet C, Franken P, *et al.* 2018**. Clock-dependent chromatin topology modulates circadian
688 transcription and behavior. *Genes & Development* **32**: 347–358.

689 **Millar AJ**. **2016**. The intracellular dynamics of circadian clocks reach for the light of ecology and
690 evolution. *Annual Review of Plant Biology* **67**: 595–618.

691 **Ming R, VanBuren R, Wai CM, Tang H, Schatz MC, Bowers JE, Lyons E, Wang M-L, Chen J,**
692 **Biggers E, *et al.* 2015**. The pineapple genome and the evolution of CAM photosynthesis.
693 *Nature Genetics* **47**: 1435–1442.

694 **Muller NA, Wijnen CL, Srinivasan A, Ryngajllo M, Ofner I, Lin T, Ranjan A, West D, Maloof JN,**
695 **Sinha NR, *et al.* 2016**. Domestication selected for deceleration of the circadian clock in
696 cultivated tomato. *Nature genetics* **48**: 89–93.

697 **Nagano AJ, Sato Y, Mihara M, Antonio BA, Motoyama R, Itoh H, Nagamura Y, Izawa T**. **2012**.
698 Deciphering and prediction of transcriptome dynamics under fluctuating field conditions. *Cell*
699 **151**: 1358–1369.

700 **Oakenfull RJ, Davis SJ**. **2017**. Shining a light on the Arabidopsis circadian clock. *Plant, Cell &*
701 *Environment* **40**: 2571–2585.

702 **Panda S, Antoch MP, Miller BH, Su AI, Schook AB, Straume M, Schultz PG, Kay SA, Takahashi**
703 **JS, Hogenesch JB**. **2002**. Coordinated transcription of key pathways in the mouse by the
704 circadian clock. *Cell* **109**: 307–320.

705 **Para A, Farré EM, Imaizumi T, Pruneda-Paz JL, Harmon FG, Kay SA**. **2007**. PRR3 Is a vascular
706 regulator of TOC1 stability in the Arabidopsis circadian clock. *The Plant Cell* **19**: 3462–3473.

707 **Ribeiro RV, Machado EC, Magalhães Filho JR, Lobo AKM, Martins MO, Silveira JAG, Yin X,**
708 **Struik PC**. **2017**. Increased sink strength offsets the inhibitory effect of sucrose on sugarcane
709 photosynthesis. *Journal of Plant Physiology* **208**: 61–69.

Ruben MD, Wu G, Smith DF, Schmidt RE, Francey LJ, Lee YY, Anafi RC, Hogenesch JB. **2018**. A database of tissue-specific rhythmically expressed human genes has potential applications in circadian medicine. *Science Translational Medicine* **10**.

Rubin MJ, Brock MT, Davis AM, German ZM, Knapp M, Welch SM, Harmer SL, Maloof JN, Davis SJ, Weinig C. **2017**. Circadian rhythms vary over the growing season and correlate with fitness components. *Molecular Ecology* **26**: 5528–5540.

Schubert V, Lermontova I, Schubert I. **2013**. The Arabidopsis CAP-D proteins are required for correct chromatin organisation, growth and fertility. *Chromosoma* **122**: 517–533.

Shalit-Kaneh A, Kumimoto RW, Filkov V, Harmer SL. **2018**. Multiple feedback loops of the Arabidopsis circadian clock provide rhythmic robustness across environmental conditions. *Proceedings of the National Academy of Sciences of the United States of America* **115**: 7147–7152.

Sharma A, Wai CM, Ming R, Yu Q. **2017**. Diurnal cycling transcription factors of pineapple revealed by genome-wide annotation and global transcriptomic analysis. *Genome Biology and Evolution* **9**: 2170–2190.

Shimizu H, Katayama K, Koto T, Torii K, Araki T, Endo M. **2015**. Decentralized circadian clocks process thermal and photoperiodic cues in specific tissues. *Nature Plants* **1**: 15163.

Sinturel F, Gerber A, Mauvoisin D, Wang J, Gatfield D, Stubblefield JJ, Green CB, Gachon F, Schibler U. **2017**. Diurnal oscillations in liver Mass and cell size accompany ribosome assembly cycles. *Cell* **169**: 651-663.e14.

Smieszek SP, Yang H, Paccanaro A, Devlin PF. **2014**. Progressive promoter element combinations classify conserved orthogonal plant circadian gene expression modules. *Journal of the Royal Society, Interface* **11**.

Song YH, Kubota A, Kwon MS, Covington MF, Lee N, Taagen ER, Laboy Cintrón D, Hwang DY, Akiyama R, Hodge SK, *et al.* 2018. Molecular basis of flowering under natural long-day conditions in Arabidopsis. *Nature Plants* **4**: 824–835.

Storch K-F, Lipan O, Leykin I, Viswanathan N, Davis FC, Wong WH, Weitz CJ. **2002**. Extensive and divergent circadian gene expression in liver and heart. *Nature* **417**: 78–83.

Takahashi N, Hirata Y, Aihara K, Mas P. **2015**. A hierarchical multi-oscillator network orchestrates the Arabidopsis circadian system. *Cell* **163**: 148–159.

Turner A, Beales J, Faure S, Dunford RP, Laurie DA. **2005**. The pseudo-response regulator Ppd-H1 provides adaptation to photoperiod in barley. *Science (New York, N.Y.)* **310**: 1031–1034.

Wang J, Nayak S, Koch K, Ming R. **2013**. Carbon partitioning in sugarcane (Saccharum species). *Frontiers in Plant Science* **4**.

Webb AAR, Seki M, Satake A, Caldana C. **2019**. Continuous dynamic adjustment of the plant circadian oscillator. *Nature Communications* **10**: 550.

Xu G. **2018**. Sensing and transport of nutrients in plants. *Seminars in Cell & Developmental Biology* **74**: 78–79.

Xu X, Hotta CT, Dodd AN, Love J, Sharrock R, Lee YW, Xie Q, Johnson CH, Webb AA. **2007**. Distinct light and clock modulation of cytosolic free Ca2+ oscillations and rhythmic CHLOROPHYLL A/B BINDING PROTEIN2 promoter activity in Arabidopsis. *Plant Cell* **19**: 3474–90.

Yang P, Wang J, Huang F-Y, Yang S, Wu K. **2018**. The plant circadian clock and chromatin modifications. *Genes* **9**.

Yeung J, Mermet J, Jouffe C, Marquis J, Charpagne A, Gachon F, Naef F. **2018**. Transcription factor activity rhythms and tissue-specific chromatin interactions explain circadian gene expression across organs. *Genome Research* **28**: 182–191.

Yeung J, Naef F. **2018**. Rhythms of the genome: circadian dynamics from chromatin topology, tissue-specific gene expression, to behavior. *Trends in Genetics* **34**: 915–926.

Zhang R, Lahens NF, Ballance HI, Hughes ME, Hogenesch JB. **2014**. A circadian gene expression atlas in mammals: implications for biology and medicine. *Proceedings of the National Academy of Sciences of the United States of America* **111**: 16219–16224.

765 **Figure Legends**

766

767 **Figure 1 – Different organs have specific sets of rhythmic transcripts in**
768 **sugarcane. (a)** The numbers of expressed and rhythmic time courses detected in leaf
769 +1 (L1), internodes 1 and 2 (I1), and internode 5 (I5) in field-grown (diel) conditions,
770 and in leaf +1 in circadian conditions (Hotta *et al.*, 2013). **(b,c)** Euler diagrams of
771 expressed time courses **(b)** and rhythmic time courses **(c)** in L1 in sugarcane in diel
772 (green) and circadian (gray) conditions. **(d)** Number of expressed time courses,
773 rhythmic time courses, and rhythmic time courses with the same phase that were found
774 specifically in L1, I1, or I5; in both L1 and I1 (L1I1, purple); in both L1 and I5 (L1I5, light
775 green); in both I1 and I5 (I1I5, orange); and in all three organs (L1I1I5, blue). In the
776 second bar, the gray area corresponds to rhythmic time courses that are expressed in
777 only one or two organs. In the third bar, the gray area corresponds to rhythmic time
778 courses in only two organs that have the same phase. The gray dashed lines show the
779 associations among bars. **(e,f)** Euler diagram of expressed and rhythmic time courses
780 in L1, I1, and I5 in field-grown sugarcane in diel conditions.

781

782 **Figure 2 – Transcripts have unique phases in different sugarcane organs. (a)**
783 Circular heatmap of the rhythmic transcript peak time (ZT0 = 0 h after dawn)
784 distribution in leaf +1 (L1), internodes 1 and 2 (I1), and internode 5 (I5). The colored
785 arrows show the times at which the most transcripts are found in each organ. The
786 times of dawn, dusk, *LHY* transcription peak, maximum light intensity, and maximum
787 temperatures are indicated by black arcs. **(b)** Proportions of transcripts that were
788 rhythmic in L1, I1, and I5 among all expressed transcripts in each organ (All), among
789 the transcripts expressed only in one organ (L1 only, I1 only, or I5 only), among the
790 transcripts expressed in two organs (L1I1, L1I5, or I1I5), and among transcripts
791 expressed in all three organs (L1I1I5). **(c)** Distribution of rhythmic transcript peak time
792 in time courses that were rhythmic in L1 but not in circadian conditions (α in Fig. 1c)
793 and rhythmic transcripts in time courses that were rhythmic in L1 and circadian
794 conditions (β). **(d)** Heatmap of functional categories that are overrepresented (shades
795 of blue) or underrepresented (shades of red) among the expressed and rhythmic
796 transcripts of L1, I1, and I5. The *P*-value was calculated using a hypergeometric test.
797 **(e)** Circular heatmap with the distribution of the peak times of rhythmic transcripts

associated with the pathways *Carbohydrate Metabolism*, *Cell Wall Synthesis & Elongation*, *Amino Acid Metabolism*, and *Transporters*.

Figure 3 – Diel rhythms of *Central Oscillator* transcripts in sugarcane organs. *LHY* **(a)**, *PRR59* **(b**), *PRR73* **(c)**, *TOC1* **(d)**, *PRR95* **(e)**, and *GI* **(f)** rhythms were measured in leaf +1 (L1, green continuous line), internodes 1 and 2 (I1, red dashed line), and internode 5 (I5, yellow dash-dotted line) of field-grown sugarcane using oligoarrays. Time courses were normalized using *Z*-score. The light-gray boxes represent the night periods.

Figure 4 – Transcripts associated with *Genetic Information Processing* have different rhythms in sugarcane organs. (a-c) Circular heatmap of the distribution of the peak time of rhythmic transcripts related to *Chromatin Remodeling* **(a)**, *Transcription Factors* **(b)**, and *Protein Synthesis* **(c)** in leaf +1 (L1, green), internodes 1 and 2 (I1, red), and internode 5 (I5, yellow). The colored arrows show the time at which the most transcripts are found in each organ. **(d-i)** Euler diagrams of all expressed transcripts **(d-f)** and rhythmic transcripts **(g-i)** in L1, I1, and I5 in field-grown sugarcane in diel conditions. **(j-l)** *SMC1* **(j**), *HB24* **(k)**, and *S15A* **(l)** rhythms measured in L1 (continuous green line), I1 (red dashed line), and I5 (yellow dash-dotted line) of field-grown sugarcane using oligoarrays. Time courses were normalized using *Z*-score. The light-gray boxes represent the night periods.

821 **Supporting Information (SI)**

822

823 **Supplemental Figure 1**

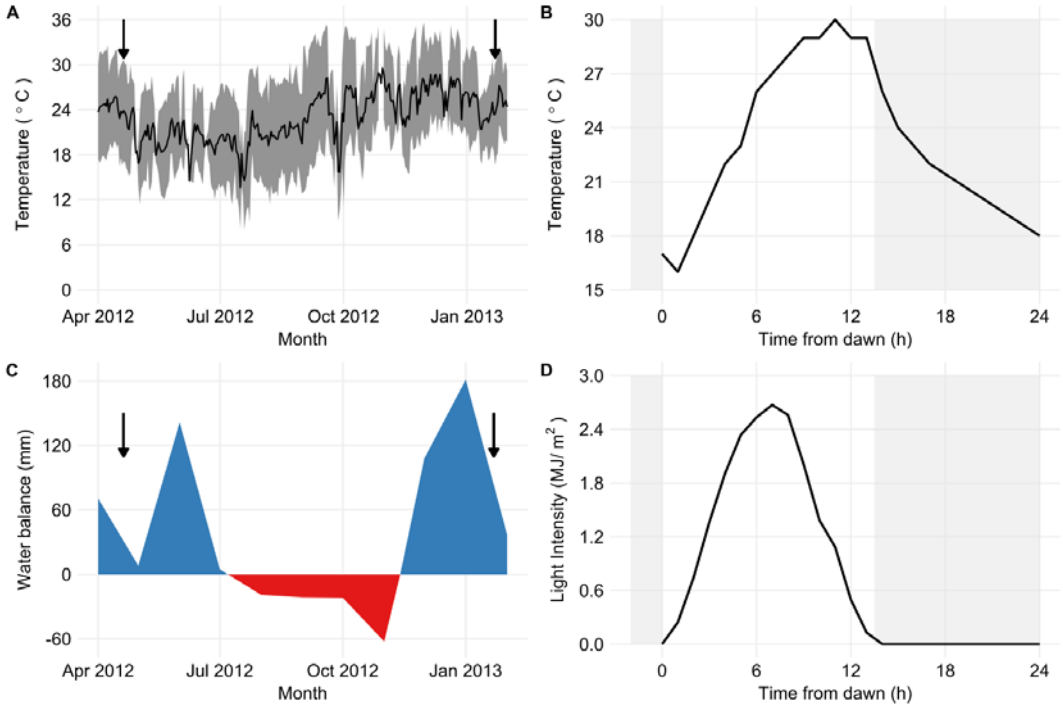

824

825 **Figure S1 – Environmental conditions in Araras (SP, Brazil).** Environmental
826 conditions during the growth period and harvesting day. **(a)** Average temperature
827 variation during the growth period (black line). The gray area shows the temperature
828 variation (maximum and minimum) during each day. The arrows show the day of
829 planting and the day of harvesting. **(b)** Temperature during the harvesting day. The
830 light-gray boxes represent the night period. **(c)** Water balance during growth period. **(d)**
831 Light intensity during the harvesting day.

832

833 **Supplemental Figure 2**

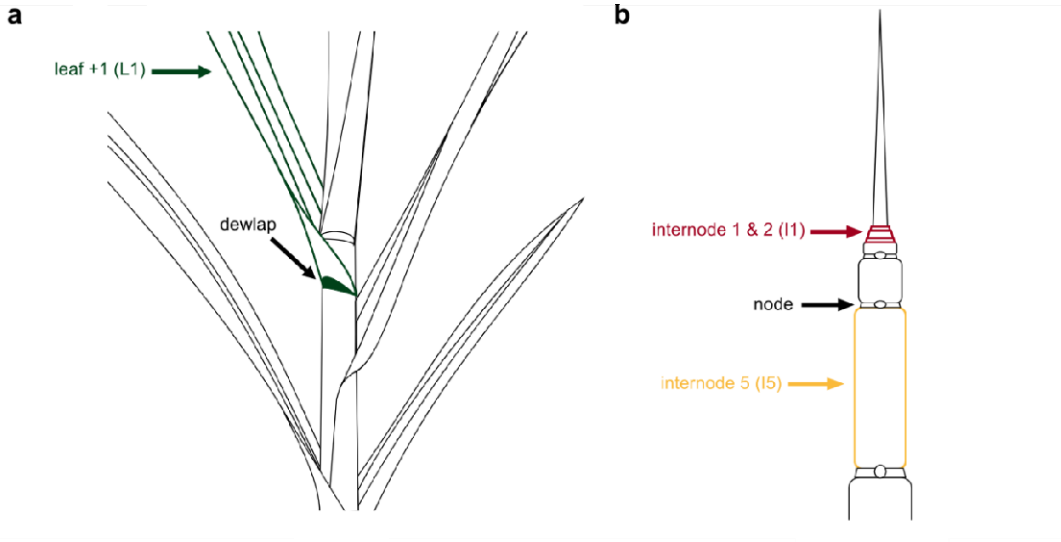

834

835 **Figure S2 – Three sugarcane organs were harvested. (a)** The leaf +1 (L1, green)
836 harvested for this study is the first leaf from the top with a clearly visible dewlap. **(b)**
837 After all of the leaves are peeled off and removed, the full stalk is exposed, so that all
838 nodes and internodes can be seen. The top two internodes (internodes 1 and 2, I1,
839 red) and the fifth internode (internode 5, I5, yellow) were also harvested.

840

841 **Supplemental Figure 3**

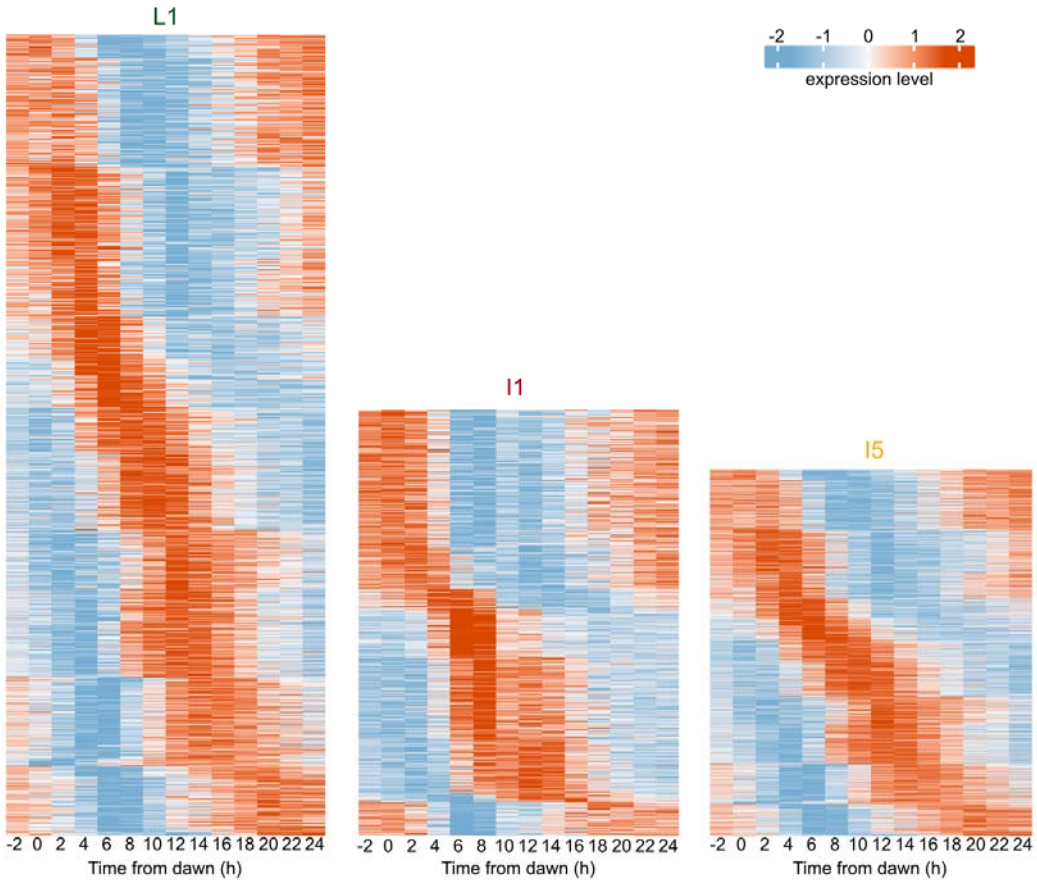

842

843 **Figure S3 – Heatmap of the expression levels of the rhythmic transcripts in**
844 **sugarcane organs.** Each line represents the time course of each rhythmic transcript in
845 leaf +1 (l1), internodes 1 and 2 (I1), and internode 5 (I5). The transcripts were
846 separated by their phase. High transcription levels are in shades of red, and low
847 transcription levels are in shades of blue. Transcription levels were normalized by *Z*-
848 score.

849

850

851 **Supplemental Figure 4**

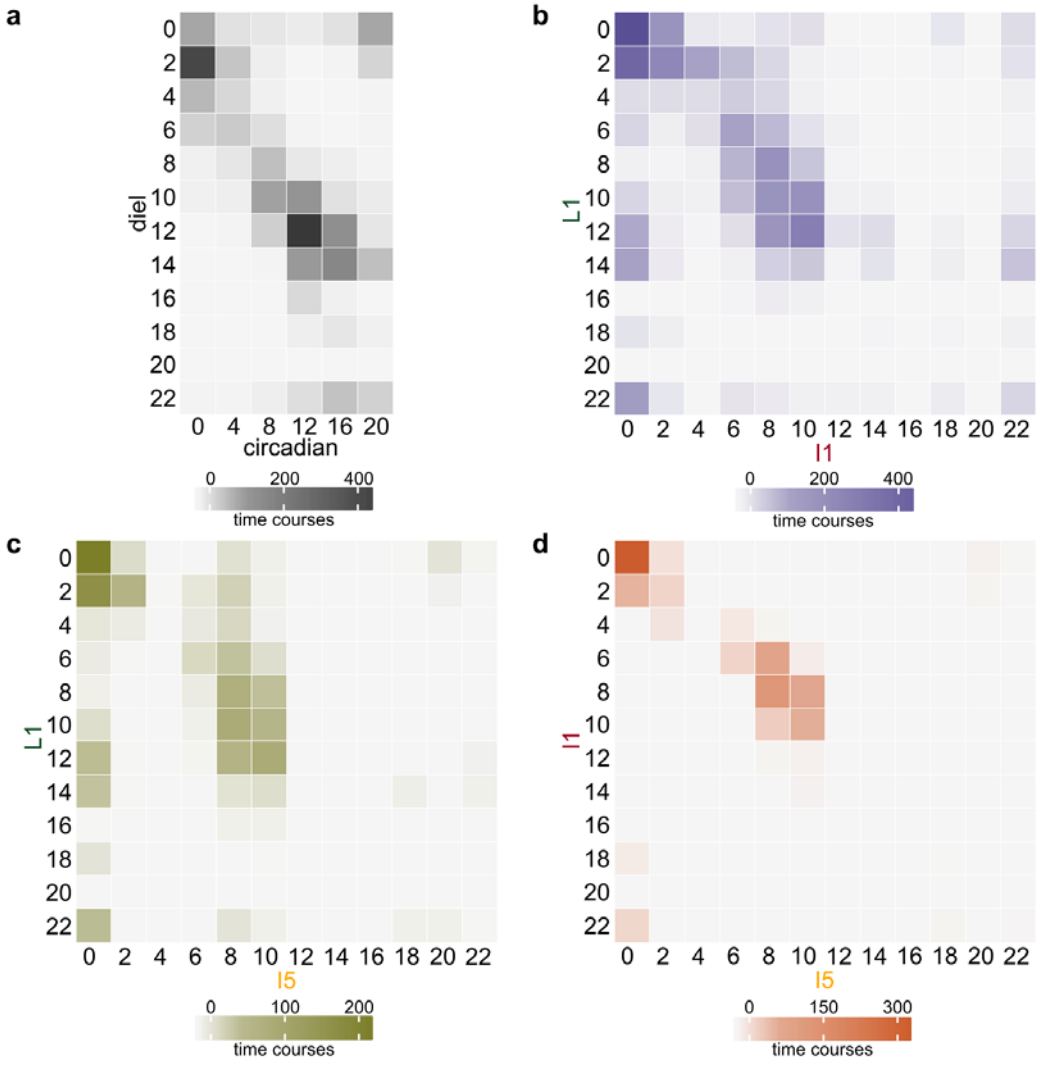

852

853 **Figure S4 – Heatmap of the phase distribution of rhythmic transcripts shared**
854 **between pairs of datasets. (a)** Phase distribution of transcripts found in leaf +1 (L1) of
855 field-grown sugarcane and L1 of sugarcane grown under circadian conditions (Hotta *et*
856 *al.*, 2013). **(b)** Phase distribution of transcripts found in L1 and internodes 1 and 2 (I1)
857 of field-grown sugarcane. **(c)** Phase distribution of transcripts found in L1 and internode
858 5 (I5) of field-grown sugarcane. **(d)** Phase distribution of transcripts found in I1 and I5
859 of field-grown sugarcane.

860

861

862 **Supplemental Figure 5**

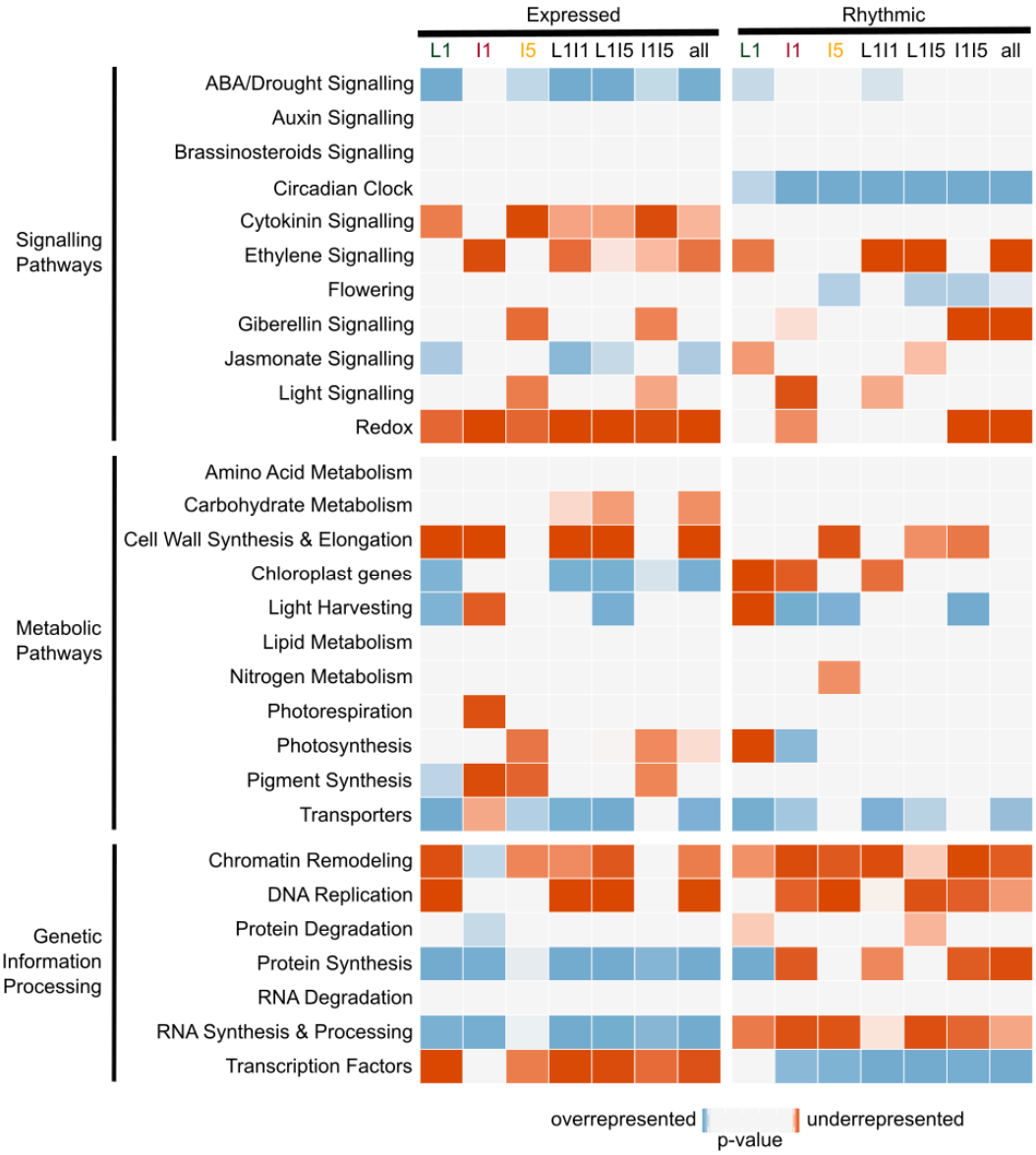

863

864 **Figure S5 –** Heatmap of functional categories that are overrepresented (shades of
865 blue) or underrepresented (shades of red) among the expressed and rhythmic
866 transcripts of L1, I1, I5, L1I1, L1I5, I1I5, and all three organs. The *P*-values were
867 calculated using a hypergeometric test.

868

869 **Supplemental Figure 6**

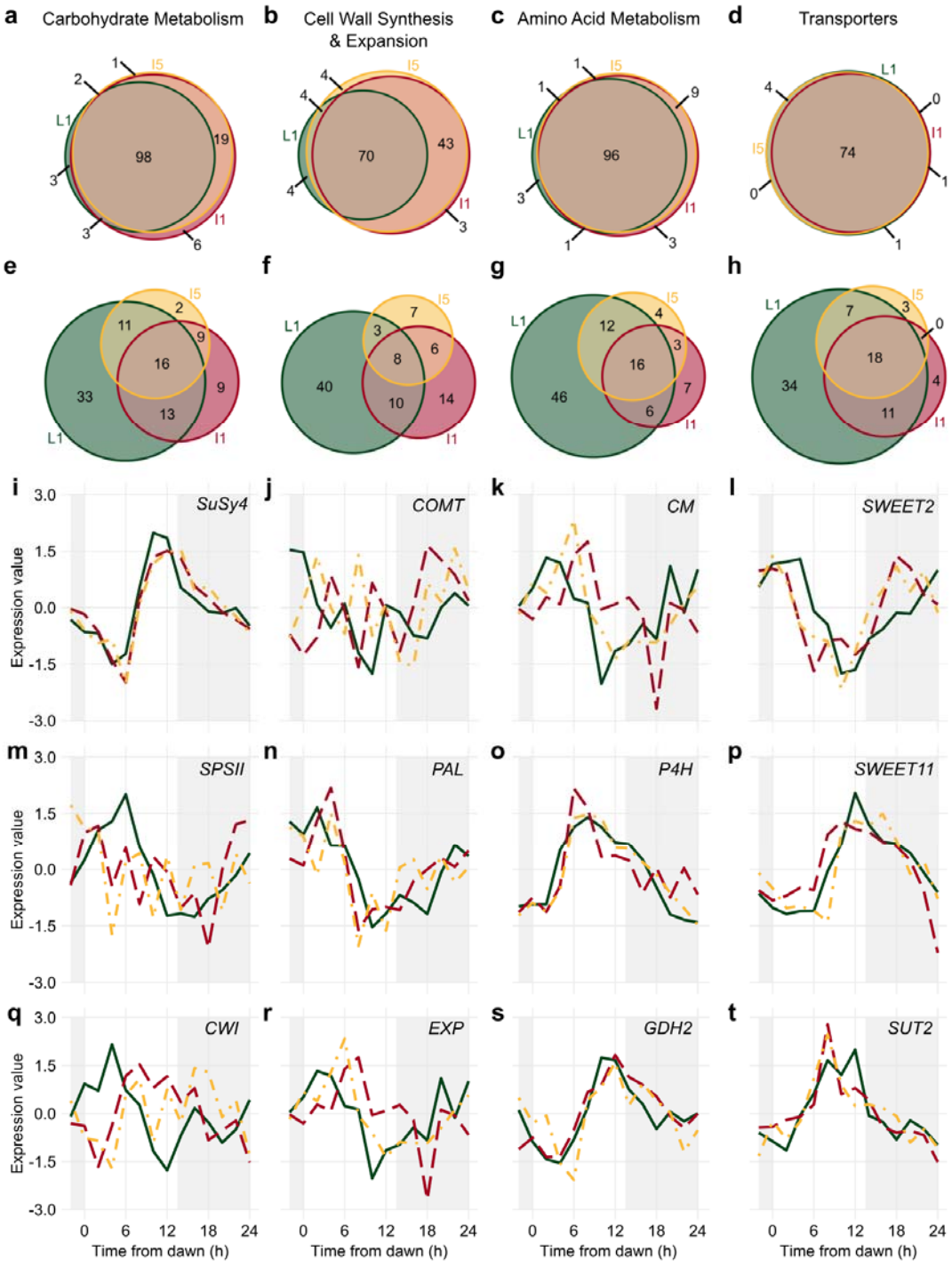

870

871 **Figure S6 – Transcripts associated with metabolic pathways have different**
872 **rhythms in sugarcane organs. (a-h)** Euler diagram of **(a-d)** expressed and **(e-h)**
873 rhythmic transcripts in leaf +1 (L1, green), internodes 1 and 2 (I1, red), and internode 5
874 (I5, yellow) in field-grown sugarcane in diel conditions. **(i-t)** Rhythms of **(i)** *SUCROSE*

875 *SYNTHASE4* (*SuSy4*), **(j)** *CATECHOL-O-METHYLTRANSFERASE* (*COMT*), **(k)**
876 *CHORISMATE MUTASE* (*CM*), **(l)** *SWEET2*, **(m)** *SUCROSE-PHOSPHATE*
877 *SYNTHASE II* (*SPSII*), **(n)** *PHENYLALANINE AMMONIA LYASE* (*PAL*), **(o)** *PROLYL*
878 *4-HYDROXYLASE* (*P4H*), **(p)** *SWEET11*, **(q)** *CELL WALL INVERTASE* (*CWI*), **(r)**
879 *EXPANSIN* (*EXP*), **(s)** *GLUTAMATE DEHYDROGENASE2* (*GDH2*), and **(t)** *SUCROSE*
880 *TRANSPORT PROTEIN2* (*SUT2*) measured in the L1 (continuous green line), I1 (red
881 dashed line), and I5 (yellow dash-dotted line) of field-grown sugarcane by oligoarrays.
882 Time courses were normalized using *Z*-score. The light-gray boxes represent the night
883 period.

884

885 **Supplemental Figure 7**

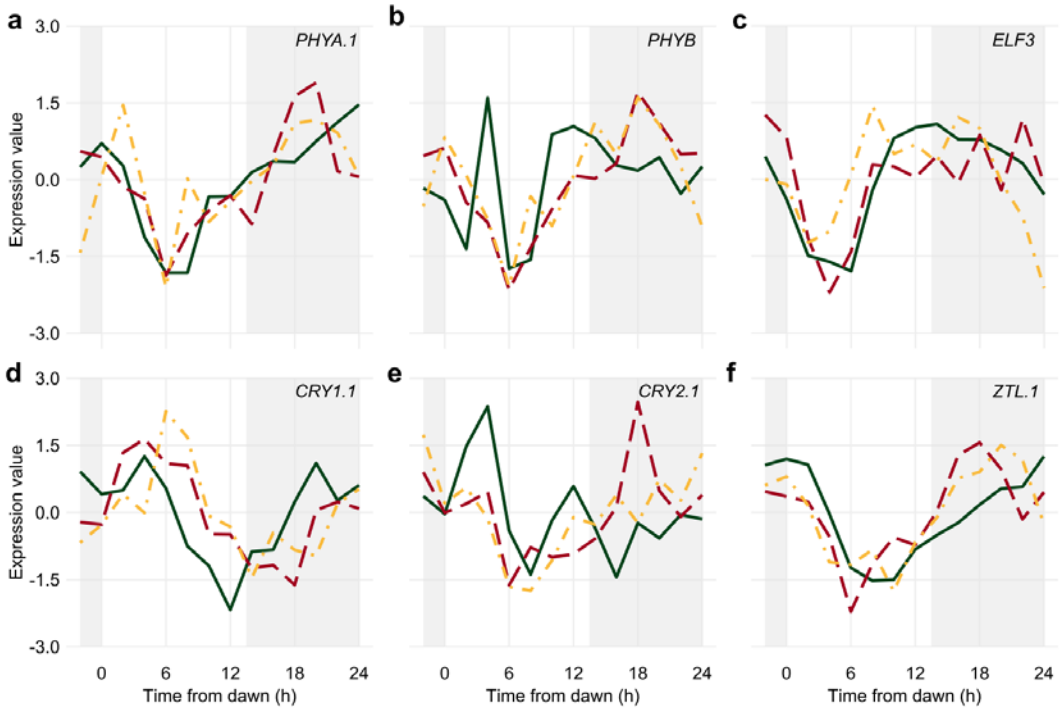

886

887 **Figure S7 – Diel rhythms of *Light Signalling* and *Central Oscillator* transcripts in**
888 **sugarcane organs.** Rhythms of **(a)** *PHYTOCHROME A.1* (*PHYA.1*), **(b)** *PHYB*, **(c)**
889 *EARLY FLOWERING3* (*ELF3*), **(d)** *CRYPTOCHROME 1.1* (*CRY1.1*), **(e)** *CRY2.1*, and
890 **(f)** *ZEITLUPE* (*ZTL*) measured in leaf +1 (L1; continuous green line), internodes 1 and
891 2 (I1; red dashed line), and internode 5 (I5; yellow dash-dotted line) of field-grown
892 sugarcane using oligoarrays. Time courses were normalized using *Z*-score. The light-
893 gray boxes represent the night period.

894

895

896 **Supplemental Figure 8**

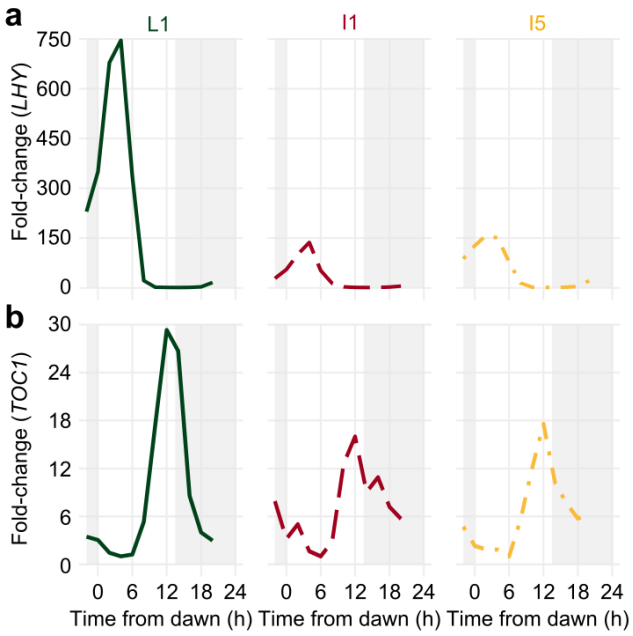

897

898 **Figure S8 – Diel rhythms of transcripts associated with the circadian clock have**
899 **different amplitudes in different sugarcane organs.** Rhythms of **(a)** *LATE*
900 *ELONGATED HYPOCOTYL* (*LHY*) and **(b)** *TIME OF CAB EXPRESSION1* (*TOC1*)
901 were measured in the leaf +1 (L1, continuous green line), internodes 1 and 2 (I1, red
902 dashed line), and internode 5 (I5, yellow dash-dotted line) of field-grown sugarcane
903 measured using RT-qPCR. *GLYCERALDEHYDE-3-PHOSPHATE DEHYDROGENASE*
904 (*GAPDH*) was used as a reference gene. Time courses were normalized by their
905 minimum value (minimum value = 1) using *Z*-score. The light-gray boxes represent the
906 night period. *LHY* primers: FWD 5′-CCACCACGGCCTAAAAGAAA-3′, RVS 5′-
907 TGGTTTTGTTGACTTGTCATTTGG-3′; *TOC1* primers: FWD 5′-
908 TTCTGCCTGAATTTGGCAAGTG-3′, RVS 5′-GGCATCGAGCACACCAATGC-3′;
909 *GAPDH* primers: FWD 5′-GGCATCGAGCACACCAATGC-3′, RVS 5′-
910 TCCTCAGGGTTCCTGATGC-3′.

911

912

913 **Supplemental Figure 9**

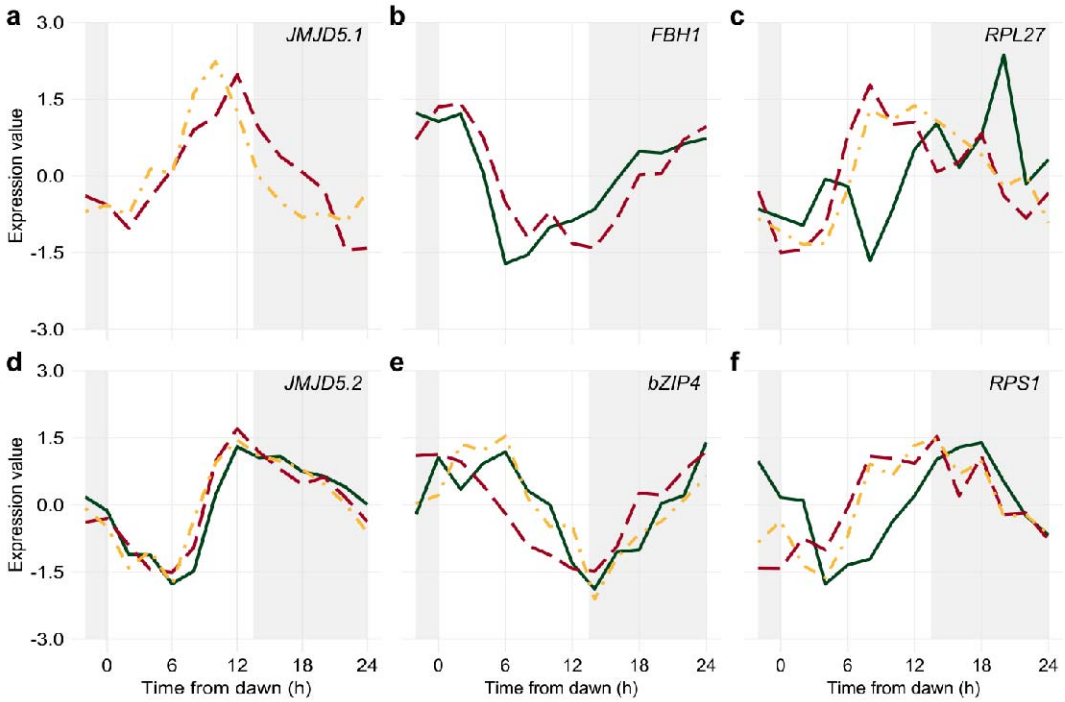

914

915 **Figure S9 – Diel rhythms of *Output Pathways* transcripts in sugarcane organs.**
916 Rhythms of **(a)** *JUMONJI-C (JMJC) DOMAIN-CONTAINING PROTEIN 5.1* (*JMJD5.1*),
917 **(b)** *FLOWERING BASIC HELIX-LOOP-HELIX1* (*FBH1*), **(c)** *RIBOSOMAL PROTEIN*
918 *L27* (*RPL27*), **(d)** *JMJD5.2*, **(e)** *BASIC LEUCINE ZIPPER4* (*bZIP4*), and **(f)** *30S*
919 *RIBOSOMAL PROTEIN S1* (*RPS1*) measured in the leaf +1 (L1, continuous green
920 line), internodes 1 and 2 (I1, red dashed line), and internode 5 (I5, yellow dash-dotted
921 line) of field-grown sugarcane by oligoarrays. Time courses were normalized using *Z*-
922 score. The light-gray boxes represent the night period.

923

924 **Supplemental Figure 10**

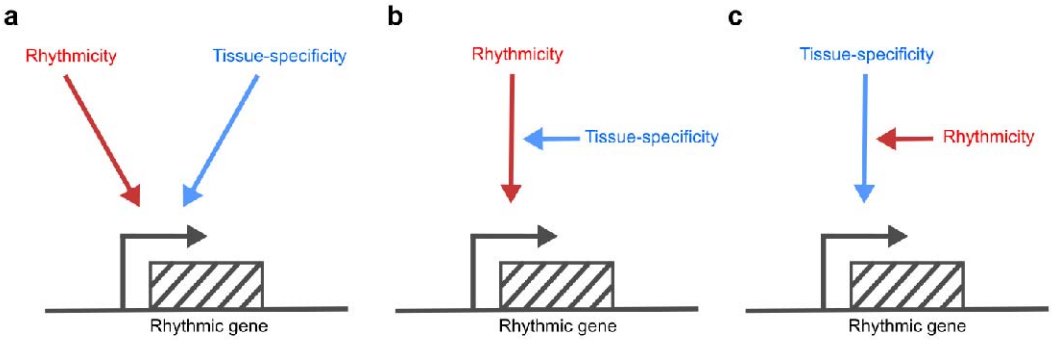

925

926 **Figure S10 – At least two different pathways are necessary to regulate tissue-**
927 **specific rhythmic transcription.** One pathway confers rhythmicity to the transcript
928 levels (red), while the other pathway confers tissue specificity (blue). These two
929 pathways could regulate transcription independently **(a)**, or one could regulate the
930 other **(b,c)**.

931

932 **Table S1 – Sugarcane genes and GenBank IDs**

Gene Symbol	Gene Name	SAS	GenBank ID
bZIP4	*BASIC LEUCINE ZIPPER 4*	SCCCCL4005C09.g	CA094172.1
CM	*CHORISMATE MUTASE*	SCCCCL4006E08.g	CA094273.1
CRY1.1	*CRYPTOCHROME 1.1*	SCRUAD1133D10.b	CA217707.1
CRY2.1	*CRYPTOCHROME 2.1*	SCRFST1042F05.g	CA178248.1
COMT	*CATECHOL-O-METHYLTRANSFERASE*	SCEQLB2018G06.g	CA262225.1
ELF3	*EARLY FLOWERING 3*	SCEZLB1009F09.g	CA113166.1
EXP	*EXPANSIN*	SCCCCL5072C04.g	CA095540.1
FBH1	*FLOWERING BASIC HELIX-LOOP-HELIX 1*	SCCCLR1022C05.g	CA119653.1
GAPDH	*GLYCERALDEHYDE-3-PHOSPHATE DEHYDROGENASE*	SCQGAM2027G09.g	CA086777.1
GDH2	*GLUTAMATE DEHYDROGENASE 2*	SCJLRT1021C04.g	CA135753.1
GI	*GIGANTEA*	SCJFAD1014B07.b	CA067312.1
HB24	*HOMEOBOX PROTEIN 24*	SCEQRT2095E01.g	CA139249.1
INV	*INVERTASE*	SCVPRT3086D06.g	CA269857.1
JMJD5.1	*JUMONJI-C (JMJC) DOMAIN-CONTAINING PROTEIN 5.1*	SCEPRZ3086F09.g	CA156744.1
JMJD5.2	*JUMONJI-C (JMJC) DOMAIN-CONTAINING PROTEIN 5.2*	SCCCLB1002G12.g	CA110901.1
LHY	*LATE ELONGATED HYPOCOTYL*	SCCCLR1048E10.g	CA167119.1
P4H	*PROLYL 4-HYDROXYLASE*	SCCCST3006H07.g	CA180585.1
PAL	*PHENYLALANINE AMMONIA LYASE*	SCEQRT1024E12.g	CA132523.1
PHYA.1	*PHYTOCHROME A.1*	SCCCCL3080H06.g	CA093547.1
PHYB	*PHYTOCHROME B*	SCQSLR1040D12.g	CA124822.1
PRR59	*PSEUDO-RESPONSE REGULATOR 59*	SCACLR1057G02.g	CA116370.1
PRR73	*PSEUDO-RESPONSE REGULATOR 73*	SCACLR1057C07.g	CA116387.1
PRR95	*PSEUDO-RESPONSE REGULATOR 95*	SCCCLR1077F09.g	CA120437.1
RPL27	*RIBOSOMAL PROTEIN L27*	SCAGLR2026E10.g	CA128063.1
RPS1	*30S RIBOSOMAL PROTEIN S1*	SCBFST3135D12.g	CA181688.1
S15A	*40S RIBOSOMAL PROTEIN S15*	SCJFRZ2007B06.g	CA151179.1
SMC1	*STRUCTURAL MAINTENANCE OF CHROMOSOMES 1*	SCEZLB1008B03.g	CA113041.1
SPSII	*SUCROSE-PHOSPHATE SYNTHASE II*	SCAGRT2037G07.g	CA137278.1
SuSy4	*SUCROSE SYNTHASE 4*	SCEPCL6023F02.g	CA097247.1
SUT2	*SUCROSE TRANSPORT PROTEIN 2*	SCEPLR1008A12.g	CA120749.1
SWEET11	*SWEET 11*	SCCCRT2002G08.g	CA137196.1
SWEET2	*SWEET2*	SCSGRT2065C08.g	CA145445.1
TOC1	*TIME OF CAB EXPRESSION 1*	SCCCSB1002H04.g	CA167119.1
ZTL.1	*ZEITLUPE*	SCCCLR1C07F05.g	CA190027.1

933 * Sugarcane Assembled Sequence.